UNCLASSIFIED

HW-78461

THE ADSORPTION OF CESIUM, STRONTIUM, AND CERIUM ON ZEOLITES FROM MULTICATION SYSTEMS

B. W. Mercer, Jr. and L. L. Ames, Jr. [1/]

Process Research and Development
Chemical Effluents Technology
CHEMICAL LABORATORY

HANFORD LABORATORIES

August 19, 1963

HANFORD ATOMIC PRODUCTS OPERATION

General Electric Company
Richland, Washington

1/ HANFORD LABORATORIES, General Electric Company, Richland, Washington

Work performed under Contract No. AT(45-1)-1350 between the Atomic Energy Commission and General Electric Company.

UNCLASSIFIED

INTERNAL DISTRIBUTION

Copy Number

1 G. J. Alkire
2 L. L. Ames
3 J. W. Barnes
4 S. J. Beard
5 O. F. Beaulieu
6 R. E. Burns
7 H. L. Caudill
8 W. J. DeMier
9 J. B. Fecht
10 W. A. Haney
11 O. F. Hill
12 R. K. Hilliard
13 E. R. Irish
14 B. F. Judson
15 R. L. Junkins
16 K. C. Knoll
17 C. E. Linderoth
18 B. W. Mercer
19 R. L. Moore
20 J. L. Nelson
21 A. M. Platt
22 H. C. Rathvon
23 W. H. Reas
24 G. L. Richardson
25 L. C. Schwendiman
26 P. W. Smith
27 W. H. Swift
28 R. E. Tomlinson
29 H. H. Van Tuyl
30 M. T. Walling
31 E. J. Wheelwright
32 File Copy
33 300 Files

EXTERNAL DISTRIBUTION

Copy Number

34 AEC, Washington
Attn: W. G. Belter

35-36 IAEA, Vienna, Austria
Attn: J. F. Honstead

37 University of North Carolina
Chapel Hill, North Carolina
Attn: H. C. Thomas

38 University of California
Berkeley 4, California
Attn: W. J. Kaufman

39 C. L. Robinson, RLOO

40 G. E. Technical Data Center
Schenectady

41 Oak Ridge National Laboratory
Attn: P. S. Baker

42-70 Extra

THE ADSORPTION OF CESIUM, STRONTIUM, AND CERIUM ON ZEOLITES FROM MULTICATION SYSTEMS

B. W. Mercer, Jr. and L. L. Ames, Jr.

INTRODUCTION

Nearly all of the fission products produced at Hanford are stored in alkaline slurries in underground waste storage tanks. Although such tank storage has been satisfactory to date, certain improvements have been proposed (1). The Chemical Processing Department has proposed to remove long-lived, heat-producing radioisotopes from the high-level wastes and package them separately for long term storage and to concentrate the residual wastes to salt cakes after a few years of liquid storage. Strontium will be removed from stored alkaline sludges by a dissolution step followed by separation, using the CSREX process(2). The cesium contained in the alkaline supernates will be separated by an ion exchange process(3) employing a cesium selective exchanger. Cesium, strontium, and rare earths will be separated from Purex denitrated waste by the CSREX process. The cesium and strontium not designated for immediate use will then be adsorbed on zeolites for a long-term storage in high integrity containers(4).

The adsorption of cesium and strontium on zeolites provides the necessary flexibility to meet immediate waste management needs and probable future market demands. The adsorbed isotopes are not readily leached by fresh water but can be recovered by eluting or leaching with suitable salt or acid solutions(5).

Since fission product recovery solutions have not been fully characterized, the results of laboratory studies based on simulated solutions are incomplete.

Therefore, methods were investigated which permit calculation of fission product loadings on zeolites from basic exchange data for a wide range of solution concentrations.

SUMMARY

Cation exchange equilibria in binary systems of Cs^{+}, Sr^{+2}, or Ce^{+3} with other cations expected in fission product recovery solutions are presented for several zeolites (Linde 4AXW, 13X, AW-400, AW-500, Norton Zeolon and clinoptilolite) along with a method of estimating zeolite loadings for multication systems. Strontium breakthrough curves are calculated from equilibrium and diffusion data for comparison with experimental breakthrough curves.

Cesium and strontium loadings of about 1.5 and 2.5 meq/g of zeolite, respectively, were obtained with cesium and strontium feed solutions. Column results show 0.9 and 1.3 meq/g of cesium and strontium, respectively, loaded together on 4A from a simulated CSREX 1BP solution.

METHODS OF INVESTIGATION

Synthetic zeolites used in these studies were obtained as pellets or crushed and sieved broken pellets. Included were sodium-based, 1/16-inch diameter pellets of 13X, 4A, 4AXW, AW-400, and AW-500 supplied by the Linde Company of Tonawanda, New York, and 1/8-inch hydrogen-based Zeolon pellets supplied by the Norton Company of Worcester, Massachusetts. The clinoptilolite was obtained from the Hector, California, deposits of the Baroid Division of National Lead. Carbonates and clays in the clinoptilolite were removed or destroyed by

a ten percent nitric acid wash prior to use. Table I gives some of the pertinent properties of the zeolites used in this study.

TABLE I

Zeolite Properties

Zeolite	SiO_2/Al_2O_3	Wt % binder	Wt % H_2O 25C	Structural type	Capacity meq/g
4A	2	20	25	A	3.5
4AXW	2	10	30	A	3.9
13X	2.8	20	25	faujasite	3.6
AW-500	4-5	25	15	chabazite	2.2
AW-400	6-7	25	12	erionite	2.0
clinoptilolite	8-10	5-15	12	clinoptilolite	1.7
Zeolon	10	---	12	mordenite	1.9

Zeolites used in the equilibrium experiments were based with saturated reagent grade chloride solutions of the desired cations. Zeolites received in the sodium form were contacted with sodium chloride solution several times to insure the purity of the sodium form. The zeolites were thoroughly washed with distilled water which was tested for chloride ion with silver nitrate solution. A final test for chloride ion was conducted on the distilled water after two days contact with the zeolite. A negative test was indicative of a minimum of NaCl inclusion.

Cation exchange capacities were determined by double tracing technique. Weighed, sodium-based zeolite samples in polyethylene bottles were contacted with a solution containing 0.1N CsCl plus 0.1N NaCl plus Cs^{134} tracer to determine cesium uptake. Cesium-based zeolites, corrected for sodium-cesium

weight differential, were then contacted with a solution containing 0.1$\underline{N}$ CsCl plus 0.1$\underline{N}$ NaCl plus Na^{22} tracer to determine sodium uptake by the same zeolites. Total zeolite capacity was assumed to be the sum of the cesium plus sodium loading. A higher capacity could have been obtained in some instances if capacities were determined with smaller size or different valence cations(6,7).

At least two days of contact time with shaking were allowed to obtain zeolite solution equilibrium. High specific activity Cs^{134}, Na^{22}, Sr^{85} and Ce^{144} were used to trace the equilibrium solutions. Solution-to-zeolite ratios were adjusted to yield statistically reliable counting rates in the equilibrium solutions. Zeolites were originally based with the untraced cation in the system. The total capacity of the zeolite minus the amount of traced cation removed from the equilibrium solution was assumed to represent the amount of traced cation on the zeolite. Eight to twelve points were determined for each ion-pair by varying the ratios of contacting cations.

Several systems were traced from both directions to confirm that equilibrium was being attained. The equilibrium solution was held at a constant total normality. Errors introduced by zeolite salt inclusion were probably less than one percent(8). A determination of equilibrium relationships in the sodium-cesium system at a total normality of 0.1 resulted in essentially the same equilibria after activity corrections, confirming that salt inclusion was not a major problem.

Zeolites used in the column experiments were sodium-based in all cases. The zeolites were crushed and sieved to obtain the desired particle size fraction.

The zeolites were washed free of dust and were air dried at room temperature.

Ion exchange columns were prepared by packing 50g of zeolite in a 1.9 cm ID diameter glass tube to a height of 21 cm. The zeolite was supported on a glass wool plug with a wire screen on top. The 50g portions of zeolite were soaked in water prior to packing in the tubes to allow air to escape from the pores of the zeolite. Five days of soaking was found adequate to remove air from particle sizes less that 1.19 mm (16 mesh, U. S. Standard). The columns were packed under water to exclude air bubbles.

Solutions were pumped downflow through the columns by means of peristaltic action pumps. Effluent samples were collected periodically for analysis. The volume of water above and below the column was subtracted from effluent volume measurements. At temperatures above 25C the columns were suspended in a controlled temperature water bath. Feed solutions were boiled to remove dissolved gases and were brought to the desired temperature in coils in the water bath before entering the columns.

RESULTS AND DISCUSSION

Equilibria

Ion exchange isotherms at 25C for binary systems containing Cs^{+}, Sr^{+2}, and Ce^{+3}, plus other ions expected in fission product recovery solutions are shown in Figures 1 through 60. The isotherms for cesium with other alkali and alkaline earth cations are generally favorable for AW-400, AW-500, Zeolon and clinoptilolite but unfavorable for 4AXW and 13X. The isotherms for strontium in the presence of sodium and calcium are favorable with 4AXW and 13X. Only

13X revealed a favorable isotherm for Ce^{+3} with alkali metal cations. The effect of temperature is not shown in this report; however, cesium adsorption generally decreases with increasing temperature[12]. Recent preliminary data indicate that strontium adsorption is slightly increased by elevating the temperature.

Plots of mass action quotients versus solution equivalent ratios are shown in Figures 61 through 74. The curves not only illustrate the large variation of the mass action quotient with solution cation concentration ratios but are useful for calculating the amount of adsorbed cations.

The mass action quotients were calculated by the following general equation:

$$K_B^A = \frac{(A_Z)^{n_A} (B_N)^{n_B}}{(B_Z)^{n_B} (A_N)^{n_A}}$$

Where A_N, B_N = Concentration of cations A and B in equivalents per liter.

A_Z, B_Z = Equivalent fractions of cations A and B on the zeolite.

n_A, n_B = Number of cations of A and B represented in the chemical equation for the exchange equilibria of A with B.

Cation Loading Estimates for Zeolites

The use of binary exchange data to predict the equilibrium distribution of cations between zeolites and process solutions is often complicated by the presence of three or more exchanging cations. Dranoff and Lapidus[9], have shown that binary exchange equilibria in dilute ternary systems (Co^{++} - H^+ -

Ag^+ and Na^+ - H^+ - Ag^+ with Dowex 50) is the same as that in pure binary systems. They concluded that this behavior makes it possible to determine equilibrium distribution in systems of more than two exchanging ions from binary exchange data.

A mass action quotient for two cations in a system containing 3 or more cations gives only the ratio of the two cations on the zeolite. Their absolute concentration cannot be estimated from this coefficient alone. However, by definition the summation of all the cation equivalent fractions on the zeolite is unity,

$$A_z + B_z + C_z \text{ - - - - - - - - - - } = 1$$

To solve for A_z, mass action expressions are substituted in place of Bz and Cz for the exchange of A with B and A with C, respectively. For example, where A and B are univalent and C is divalent the following equation is obtained:

$$A_z + \frac{(B_N)}{(K_B^A)\ (A_N)}\ A_z + \frac{(C_N)}{(K_C^A)\ (A_N)^2}\ A_z^2 = 1$$

Cesium and strontium loadings estimated from binary exchange data are compared with experimental column values for various solutions and zeolites in Table II. When several column values were available for the same feed and zeolite, the data for the small particle size and/or the slow flow rate were selected because of a closer approach to equilibrium. The column values were calculated from the volume of solution to 50 percent breakthrough of the Cs^+ or Sr^{+2} on a log-probability plot, except where marked by an asterisk (*). The latter were calculated from breakthrough curves by integrating from C/C_o to 1. In these cases the effluent

Sr^{+2} exceeded 100 percent breakthrough as the column approached equilibrium with the feed solution. Part of the strontium was desorbed from the column as the zone of sorbed cesium spread throughout the column.

Solutions No. 1 and 2 in Table II simulate ion exchange recovery solutions[10] of cesium from stored high-level waste supernatant solutions. Solution No. 1 has a higher Na:Cs ratio than that expected for the ion exchange process in addition to K^+ and NH_4^+ impurities. Solution No. 3 is a simulated D2EHPA[1] process 1BP solution[11] (treated for acid removal and pH adjustment). The D2EHPA process was initially considered for strontium and rare earth separation but was later replaced by the CSREX process. Strontium recovered by the CSREX process will have more calcium impurity than that of the D2EHPA process. Solutions No. 4 and 5 are simulated CSREX process 1BP solutions[10] (treated for acid removal and pH adjustment). Solution No. 4 has a higher Na^+ concentration than that anticipated for the CSREX process.

Except for Solution No. 5 and 4A and AW-400 the estimated and experimental results generally agree within experimental error. The cause for the differences for solution No. 5 and 4A and AW-400 are unknown at the present time. It is possible that the 50 percent breakthrough estimates are in error because of some very slow exchange taking place.

Initial results with solutions containing high concentrations of sodium carbonate to cesium carbonate indicated that activity corrections would be necessary to obtain satisfactory cesium loading estimates on zeolites. However, subsequent work with solutions in the expected concentration range for fission product packaging

---

[1] Di(2-ethyl-hexyl) phosphoric acid

TABLE II

Comparison of Estimated Cesium and Strontium Loadings with Experimental Loadings at 25C

Solution No.	Zeolite	Cation Concentrations in Gram Equivalents per Liter						Common Anion	Sorbed Cation	Estimated Loading meq/g	Experimental Loading meq/g
		Cs^+	Sr^{+2}	Na^+	Ca^{+2}	K^+	NH_4^+				
1	AW-400	0.056	--	1.00	--	0.025	0.010	$CO_3^=$	Cs^+	1.18	1.25
2	AW-400	0.08	--	0.64	--	--	--	"	Cs^+	1.50	1.51
2	AW-500	"	--	"	--	--	--	"	Cs^+	1.54	1.40
2	Zeolon	"	--	"	--	--	--	"	Cs^+	1.33	1.35
2	Clinoptilolite	"	--	"	--	--	--	"	Cs^+	1.50	1.42
3	4A	--	0.070	0.20	0.020	--	--	NO_3	Sr^{+2}	2.70	2.50
4	4A	0.040	0.054	1.17	0.054	--	--	"	Sr^{+2}	1.37	1.18
4	4A	"	"	"	"	--	--	"	Cs^+	0.25	0.27
4	AW-400	"	"	"	"	--	--	"	Cs^+	0.98	1.06
4	AW-500	"	"	"	"	--	--	"	Cs^+	1.08	1.11
5	4A	0.040	0.054	0.20	0.054	--	--	"	Sr^{+2}	1.76	1.30
5	4A	"	"	"	"	--	--	"	Cs^+	0.47	0.90
5	AW-400	"	"	"	"	--	--	"	Sr^{+2}	0.16	0.08*
5	AW-400	"	"	"	"	--	--	"	Cs^+	1.14	1.45
5	AW-500	"	"	"	"	--	--	"	Sr^{+2}	0.07	0.07*
5	AW-500	"	"	"	"	--	--	"	Cs^+	1.34	1.33
5	Clinoptilolite	"	"	"	"	--	--	"	Cs	1.07	1.13

*See Text - Page 9

show that activity corrections do not significantly improve the accuracy of the loading estimates.

Recent preliminary data indicate that the Sr-Ca and Sr-Na equilibria with 4A is only slightly different at 70C compared with data at 25C. Thus, approximate 4A loadings at 70C may be predicted for Na-Sr-Ca systems from mass action quotients determined at 25C.

Column Studies

Because of the generally slower exchange rate of strontium relative to cesium the variables affecting the rate of strontium uptake were studied in greater detail[13]. Most of this work involved 4A zeolite and simulated D2EHPA TBP solutions. The 4A zeolite is the most selective for strontium in the presence of sodium of the zeolites studied. Figures 75 through 81 show the effect of particle size, temperature, flow rate and column length on the strontium breakthrough curves. In general, increasing the temperature and decreasing the particle size will reduce the loading cycle time and the amount of recycle effluent. Decreasing the flow rate will reduce the amount of recycle effluent but will increase loading time. (Column effluent containing significant concentrations of strontium will be recycled to the headend of the recovery process). Column length had no significant effect on the slope of the strontium breakthrough curve for the experimental conditions given.

Very small particle sizes are undesirable because of the high pressure drops across the bed of zeolite during drying[14]. The physical properties of the 8 x 12

mesh beads and 1/16-inch pellets of 4A are superior to the crushed material but loading and drying time are believed to be too long for process use.

Table III shows the amount of strontium adsorbed at various column throughput values for the curves in Figure 77.

Cesium breakthrough curves for cesium selective zeolites and simulated ion exchange recovery solutions are shown in Figures 82 through 83. The solutions containing 0.32M Na_2CO_3 and 0.04M Cs_2CO_3 represent about the maximum Na:Cs ratio desired if a minimum loading of 1.5 meq of cesium per gram of zeolite is to be achieved.

TABLE III

Strontium Loading of 4A Zeolite

Particle Size	Strontium Loading meq/g				
Mesh	30 c.v.	35 c.v.	40 c.v.	45 c.v.	50 c.v.
16-18	2.10	2.29	2.38	2.49	2.60
20-25	2.33	2.53	2.65	2.72	2.77
30-35	2.43	2.61	2.69	2.71	2.76
45-50	2.47	2.70	2.79	2.80	2.86
Flow rate 12 c.v./hr*					

*c.v. = Column Volume, includes volume of zeolite plus interstitial solution.

Cesium and strontium breakthrough curves for columns of 4A and a simulated CSREX 1BP feed solution are shown in Figure 87. Although the cesium and strontium break through about the same time, the cesium approaches $C/C_o = 1$ more rapidly than strontium.

Cesium breakthrough curves for AW-400, AW-500 and clinoptilolite with CSREX 1BP feed are shown in Figure 88. Cesium loading on AW-400 and AW-500 is about 95

percent of the total cesium plus strontium loading. If desired, the purity of the cesium could probably be increased by removing the strontium with a scrub solution containing a suitable complexing agent.

The strontium breakthrough curves for AW-400 and AW-500 with CSREX 1BP feed are shown in Figure 89. The strontium exceeds $C/C_o = 1$ because cesium replaces the initially-adsorbed strontium.

Cesium and strontium breakthrough curves for 4A at 80C with CSREX 1BP feed are shown in Figure 90.

The addition of citrate ion to feed solutions containing Sr^{90} and rare earths is believed desirable to complex the Y^{90} and rare earths. If the Y^{90} and Ce^{144} are not complexed, these isotopes may adsorb in a narrow band at the influent end of the column and cause heating problems at this point. A concentration of 0.005 molar citrate in the D2EHPA 1BP feed solutions was found sufficient to prevent significant adsorption of Y^{+3} and Ce^{+3}. The Y^{+3} K_d increases for concentrations of citrate ion below 0.005M with simulated D2EHPA 1BP solutions.

Application of Plate Theory to Column Operation

The method of Gleuckauf [15,16] was used to calculate theoretical cesium and strontium breakthrough curves for columns of zeolites. This method is approximate because of the simplifying assumptions made in deriving the equations. For ordinary ion exchange work the height of a theoretical plate (Δ) may be calculated as follows:

$$\Delta = 1.64\ r + \frac{\delta}{(\delta + \beta)^2} \cdot \frac{0.142\ r^2\ \overline{F}}{D_S} + \left(\frac{\delta}{\delta + \beta}\right)^2 \frac{0.266\ r^2 \overline{F}}{D_L(1 + 70\ r\ \overline{F})}$$

Where: δ = amount of adsorbed cations per cm^3 of zeolite divided by amount of cation per ml of solution in equilibrium with the zeolite,

r = radius of particle in cm,

$\bar{F}$ = linear flow velocity of feed solution above the bed (cm/sec),

D_S = particle diffusion coefficient (cm^2/sec),

D_L = liquid diffusion coefficient (cm^2/sec) and

β = void fraction of the column.

The number of theoretical plates (N) is:

$$N = \frac{\text{Column height}}{\Delta} = \frac{(V_{0.5})\ (V_{0.159})}{(V_{0.5} - V_{0.159})^2}$$

Where $V_{0.5}$ = effluent volume at $C/C_o = 0.5$

$V_{0.159}$ = effluent volume at $C/C_o = 0.159$

Curves of D_L and D_S for strontium as a function of temperature with simulated D2EHPA 1BP solution and 4A zeolite are shown in Figure 91. The method of Vinograd and McBain[17] was used to calculate the strontium D_L curve from conductance data[18]. Counter diffusion of 0.07N Sr^{+2} and 0.02N Ca^{+2} with Na^+ (0.09N concentration gradient) was assumed. Approximate transference numbers used for calculating ionic conductance values for Na^+, Sr^{+2}, and Ca^{+2} in nitrate solutions were 0.42, 0.45, and 0.45 respectively. The D_S curve is plotted through D_S values calculated from Glueckauf's equations using some of the column data in Figures 75 through 81 and other column data not shown. Data yielding plate heights less than 1 cm were not used because of the apparent

inaccuracy of the resulting D_S values. The data from columns having less than 3 theoretical plates were also not used.

Reducing the flow rate and particle size tends to increase the D_S values. Considerable variation in duplicate results probably reflect aberrations in column operation (e.g., channeling).

Figures 92, 93 and 94 show calculated and experimental strontium breakthrough curves with 4A and simulated D2EHPA feed. An example of the calculation involved for the curve in Figure 92 is given in the Appendix. At a flow rate of 12 c.v./hr and room temperature, the experimental $C/C_o = .5$ occurs at less volume than at 80C. Although the higher temperature may cause a slight shift in equilibrium towards higher strontium loading, most of the difference is believed due to kinetics. Both decreasing flow rate and smaller particle size will normally give somewhat greater effluent volume to $C/C_o - .5$.

ACKNOWLEDGMENT

The authors wish to acknowledge the help and suggestions of Mrs. Olevia C. Sterner and Mr. R. G. Parkhurst in carrying out the many experiments involved in this work.

REFERENCES

1. Tomlinson, R. E. Hanford High-Level Waste Management, HW-SA-2515, October, 1962.

2. Irish, E. R. Quarterly Progress Report - Research and Development Activities-Fixation of Radioactive Residues, HW-77299, January-March, 1963.

3. Nelson, J. L. and B. W. Mercer. Ion Exchange Separation of Cesium from Alkaline Waste Supernatant Solutions, HW-76449. January, 1963.

4. Swift, W. H. Fission Product and Waste Packaging by Inorganic Zeolite Adsorption, HW-73694. June, 1962.

5. Knoll, K. C. The Effect of Heat on Vaporization and Elution of Sr^{85} and Cs^{137} Adsorbed on Zeolites, HW-77830. July, 1963.

6. Barrer, R. M. and W. M. Meier, Exchange Equilibria in a Synthetic Crystalline Exchanger, Trans. Faraday Soc., 55, 1959.

7. Barrer, R. M. and D. C. Sammon. Exchange Equilibria in Crystals of Chabazite, Jour. Chem. Soc. London, 2838-2849, 1955.

8. Barrer, R. M. and W. M. Meier. Structural and Ion Sieve Properties of a Synthetic Crystalline Exchanger. Trans. Faraday Soc., 54, 1958.

9. Dranoff, J. and L. Lapidus. Equilibrium in Ternary Ion Exchange Systems, Ind. Eng. Chem., 49, 1297-1302, 1957.

10. Smith, P. W. Personal Communication. April, 1963.

11. Richardson, G. L. Personal Communication. July, 1962.

12. Ames, L. L. Jr. Some Zeolite Equilibria with Alkali Metal Cations, HW-SA-3031. April, 1963.

13. Ames, L. L. Jr. and K. C. Knoll. Loading and Elution Characteristics of Some Natural and Synthetic Zeolites, HW-74609. August, 1962.

14. DeMier, W. V. Personal Communication. July, 1963.

15. Glueckauf, E. Principles of Operation of Ion Exchange Columns, Soc. Chem. Ind. Monograph I, Ion Exchange and its Applications, 34-56, 1955.

16. Glueckauf, E. Theory of Chromotography, Part 9, The "Theoretical Plate" Concept in Column Separations, Trans. Faraday Soc., 51, 34-38, 1955.

17. Vinograd, J. R. and J. W. McBain. Diffusion of Electrolytes and of Their Ions in Mixtures. Jour. Am. Chem. Soc., 63, 1941.

18. Landolt-Bornstein. 6 Auflage, Zahlenwerte Und Funktionen, II Band, 7 Teil.

APPENDIX

Sample calculation for theoretical strontium breakthrough curve in Figure 92.

Experimental Conditions

Feed	- 0.04 M $NaNO_3$, 0.007 M $Sr(NO_3)_2$, 0.002 M $Ca(NO_3)_2$.
Particle size	- 0.027 cm average radius, (20 x 50 mesh U. S. Standard).
Column size	- 1.9 cm diameter, 21 cm height.
Packed density	- 0.83 g/cm^3.
Flow rate	- 60 c.v./hour ($\bar{F}$ = 0.353 cm/sec).
Temperature	- 80C.
Exchanger weight	- 50g.
Zeolite	- 4A

The equilibrium loading is determined from 4AXW data given in Figures 69 and 70.

$$\frac{(Na_N)^2}{Sr_N} = \frac{0.0016}{0.014} = 0.11, \quad K_{Na}^{Sr} = 6$$

and

$$\frac{(Ca_N)}{(Sr_N)} = \frac{0.004}{0.014} = 0.29, \quad K_{Na}^{Sr} = 2.8$$

The equation for determining Sr_z is:

$$Sr_z + \sqrt{\frac{(Na_N)^2}{(K_{Na}^{Sr})\ (Sr_N)}\ Sr_z} + \frac{(Ca_N)}{(K_{Ca}^{Sr})\ (Sr_N)}\ Sr_z = 1$$

which after numerical substitution becomes:

$$Sr_z + \sqrt{\frac{0.11}{6}\ Sr_z} + \frac{0.29}{2.8}\ Sr_z = 1.$$

The equation is then reduced to:

$$1.22\ Sr_z^2 - 2.22\ Sr_z + 1 = 0.$$

The solution to this is:

$$Sr_z = 0.79$$

The strontium loading is:

$$0.79 \times 3.5\ ^{meq}/_{g} = 2.8\ ^{meq}/_{g}.$$

Then

$$\delta = \frac{(2.8\ ^{meq}/_{g})\ (0.83\ ^{g}/_{cm^3})}{0.014\ ^{meq}/_{ml}} = 166\ ^{ml}/_{cm^3}$$

The height of a theoretical plate is:

$$\Delta = (1.64)(0.0271) + \frac{(166)}{(166 + 0.4)^2} \cdot \frac{(0.142)(0.0271)^2}{5.2 \times 10^{-7}} (0.353) + \left(\frac{166}{166 + 0.4}\right)^2 \frac{(0.266)(0.0271)^2(0.353)}{1.83 \times 10^{-5}\ [1 + (70)(0.0271)(0.353)]}$$

$$\Delta = 2.7 \text{ cm.}$$

The number of theoretical plates is:

$$N = \frac{\text{Column height}}{\text{Plate height}} = \frac{21 \text{ cm}}{2.7 \text{ cm}} = 7.8$$

The number of column volumes to $C/C_o = 0.5$ is:

$$V_{0.5} = \delta + \beta = 166 \quad (\beta \text{ is insignificant in this case})$$

Now,

$$N = \frac{(V_{0.5})\ (V_{0.159})}{(V_{0.5} - V_{0.159})} = 7.8 = \frac{(166)(V_{0.159})}{(166 - V_{0.159})^2}$$

which reduces to:

$$V^2_{0.159} - 354\ V_{0.159} + 27556 = 0.$$

The solution to this is:

$$V_{0.159} = 116$$

A straight line drawn through the points $V_{0.5}$ and $V_{0.159}$ on log-probability graph paper (erf^{-1} [2 C/C_o - 1] vs. log column volumes) will yield the theoretical strontium breakthrough curve in Figure 92.

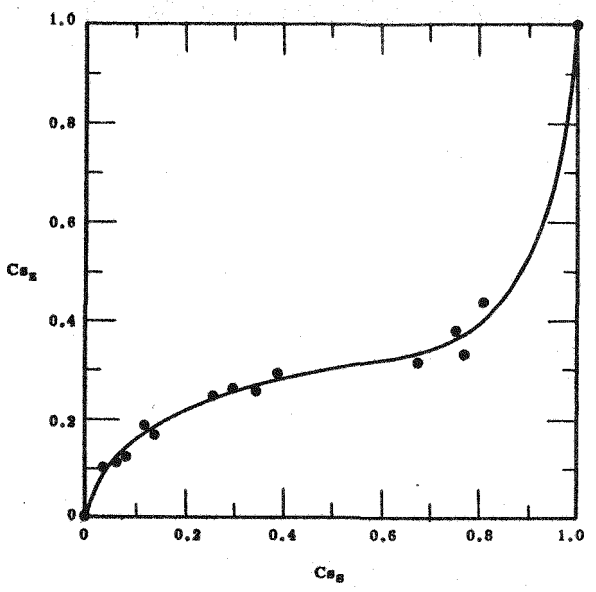

Figure 1

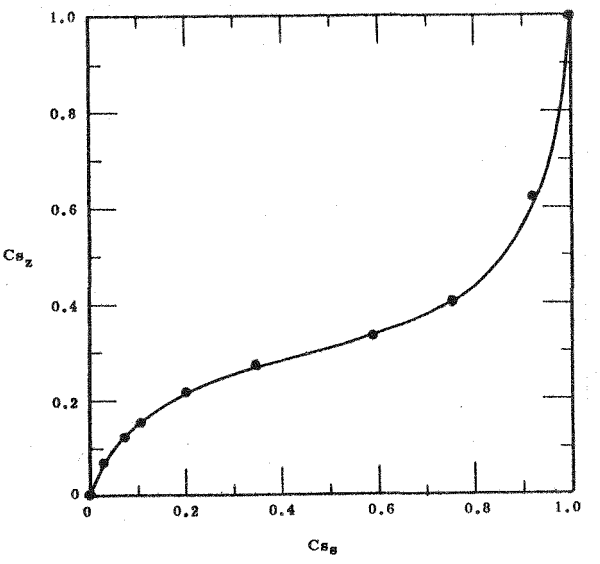

Figure 2

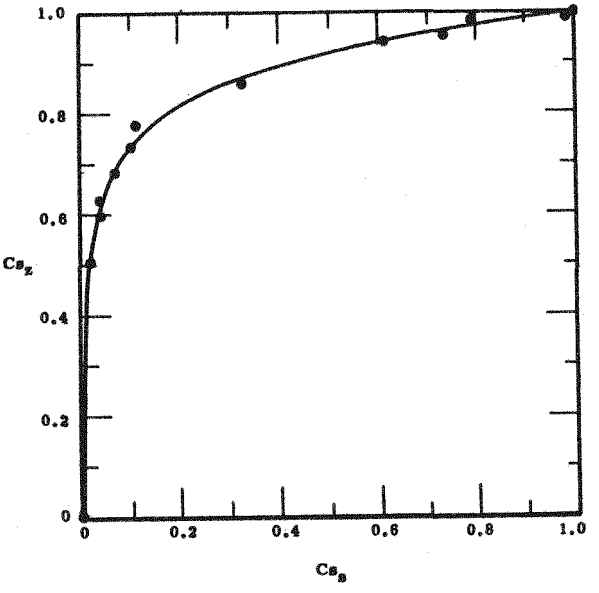

Figure 3

Figures 1, 2 and 3. The 25C isotherm for the reaction $Na_z + Cs_s = Cs_z + Na_s$ with 4AXW, 13X, and AW-400, respectively. Total equilibrium solution normality was constant at one.

Cs_z = Equivalent fraction of cesium on the zeolite.
Cs_s = Equivalent fraction of cesium in the equilibrium solution.

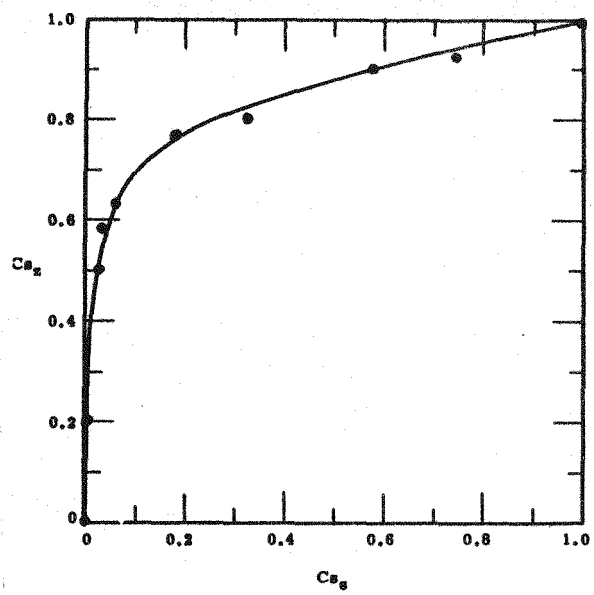

Figure 4

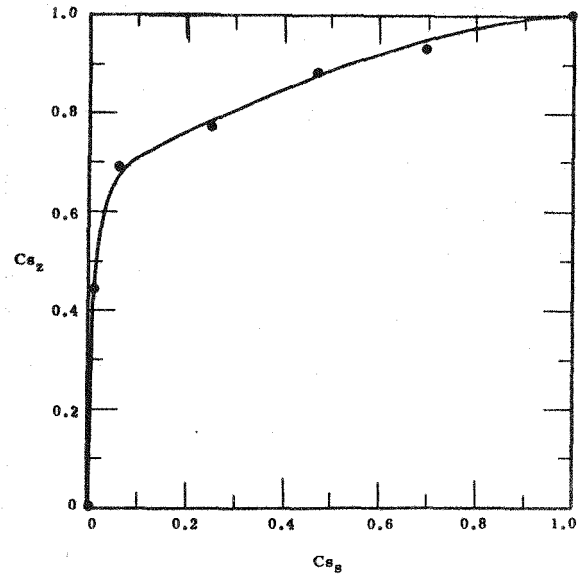

Figure 5

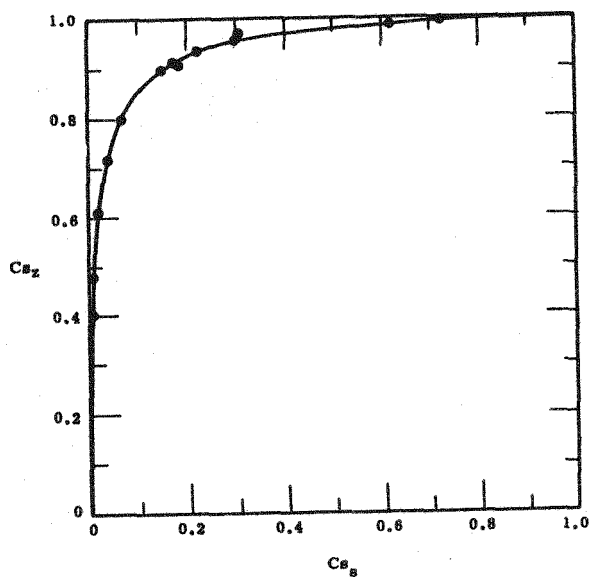

Figure 6

Figures 4, 5 and 6. The 25C isotherm for the reaction $Na_z + Cs_s = Cs_z + Na_s$ with AW-500, Zeolon, and clinoptilolite, respectively. Total equilibrium solution normality was constant at one.

Cs_z = Equivalent fraction of cesium on the zeolite.
Cs_s = Equivalent fraction of cesium in the equilibrium solution.

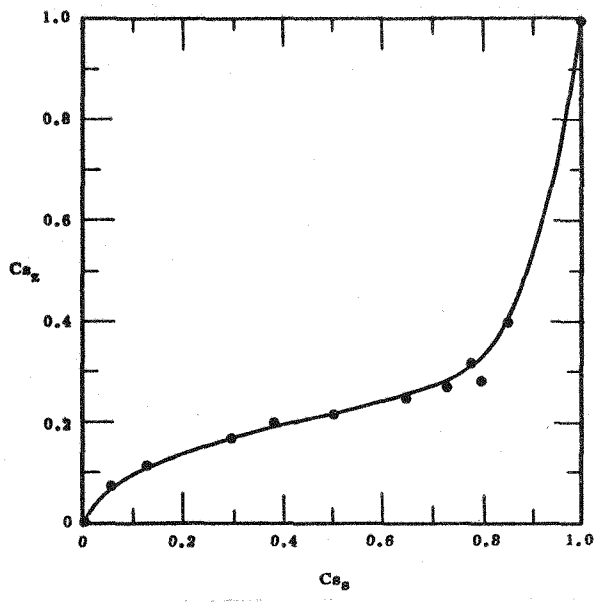

Figure 7

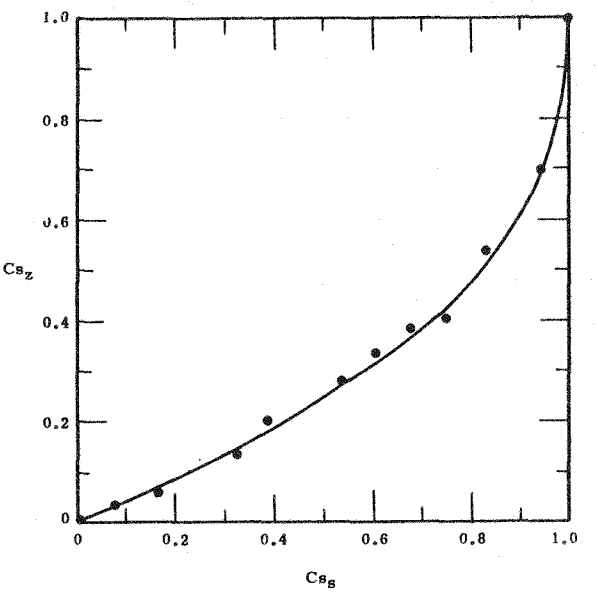

Figure 8

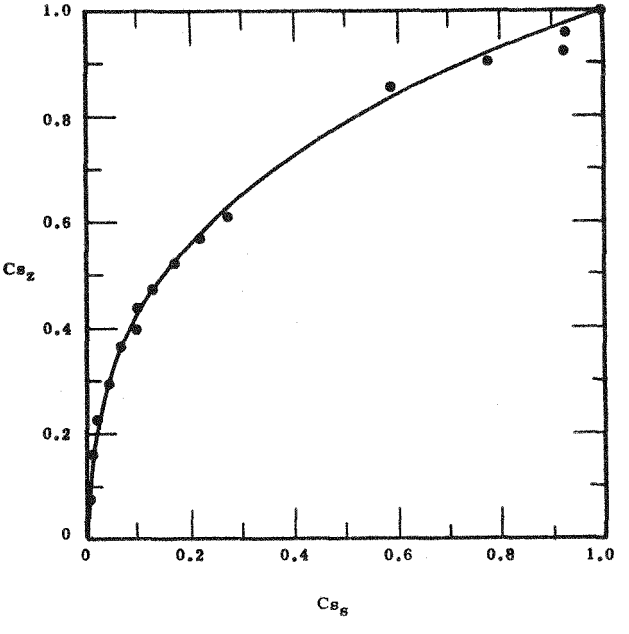

Figure 9

Figures 7,8 and 9. The 25C isotherm for the reaction $K_z + Cs_s = Cs_z + K_s$ with 4AXW, 13X, and AW-400, respectively. Total equilibrium solution normality was constant at one.

Cs_z = Equivalent fraction of cesium on the zeolite.
Cs_s = Equivalent fraction of cesium in the equilibrium solution.

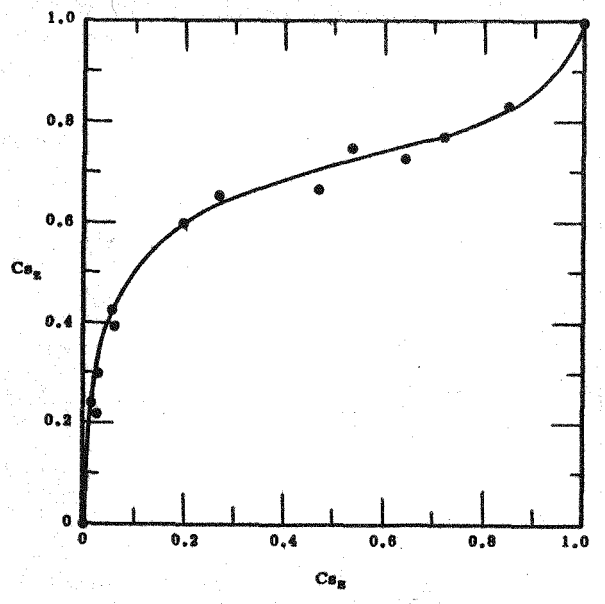

Figure 10

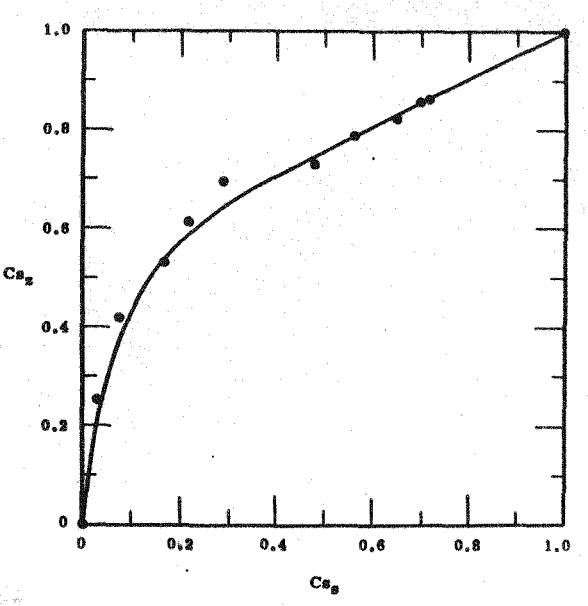

Figure 11

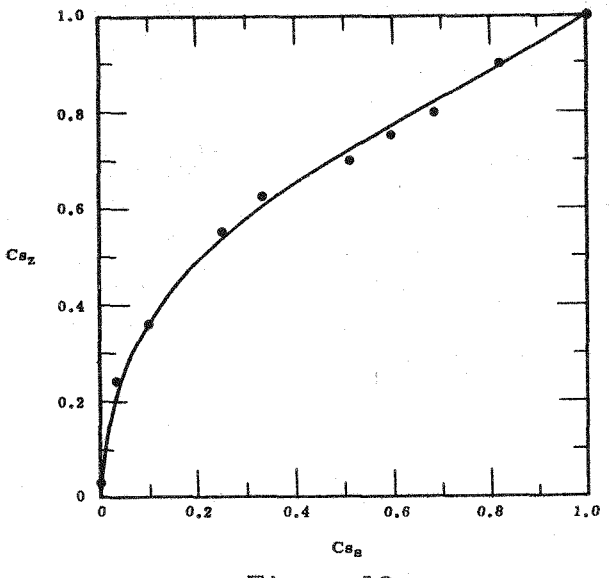

Figure 12

Figures 10, 11 and 12. The 25C isotherm for the reaction $K_z + Cs_s = Cs_z + K_s$ with AW-500, Zeolon, and clinoptilolite, respectively. Total equilibrium solution normality was constant at one.

Cs_z = Equivalent fraction of cesium on the zeolite.
Cs_s = Equivalent fraction of cesium in the equilibrium solution.

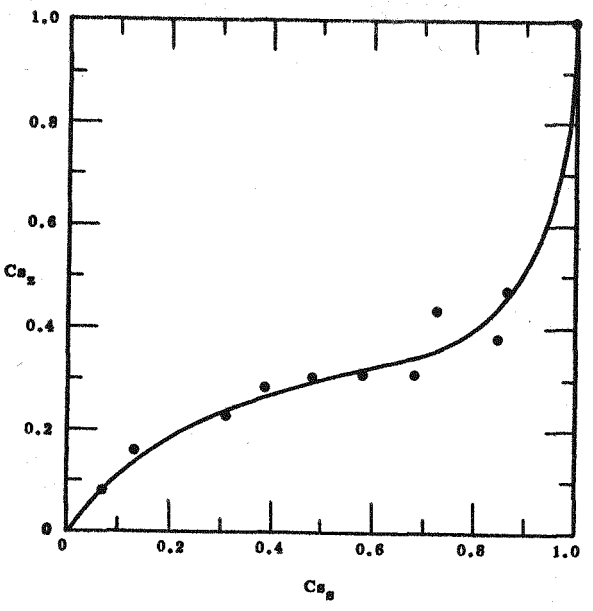

Figure 13

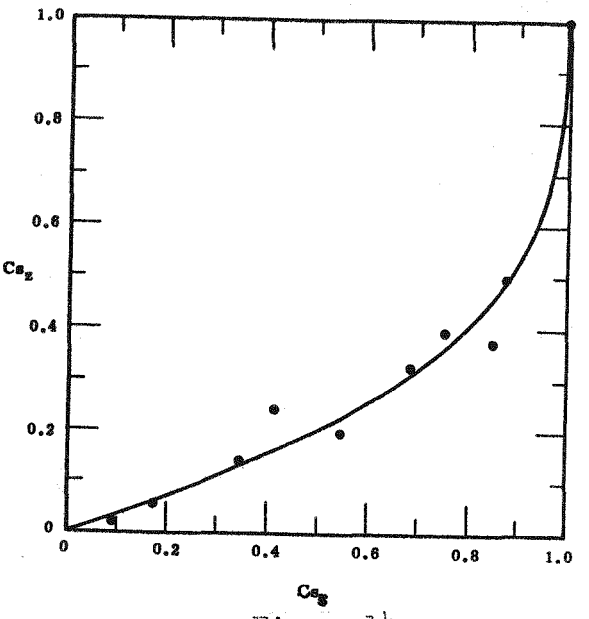

Figure 14

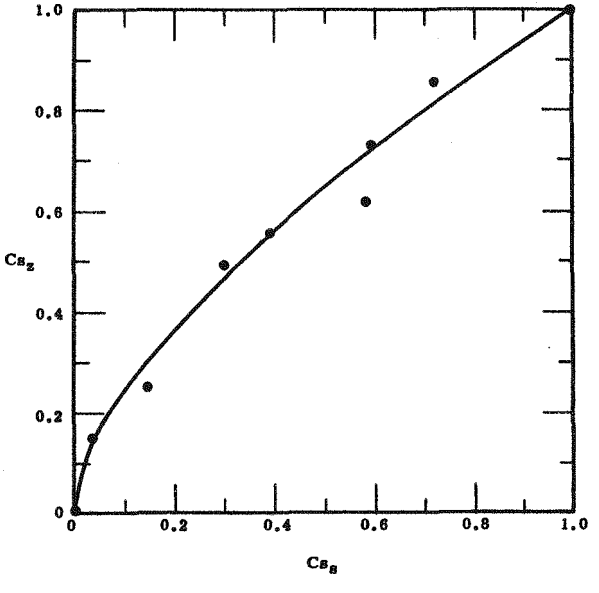

Figure 15

Figures 13, 14 and 15. The 25C isotherm for the reaction $Rb_z + Cs_s = Cs_z + Rb_s$ with 4AXW, 13X, and AW-400, respectively. Total equilibrium solution normality was constant at 0.5.

Cs_z = Equivalent fraction of cesium on the zeolite.
Cs_s = Equivalent fraction of cesium in the equilibrium solution.

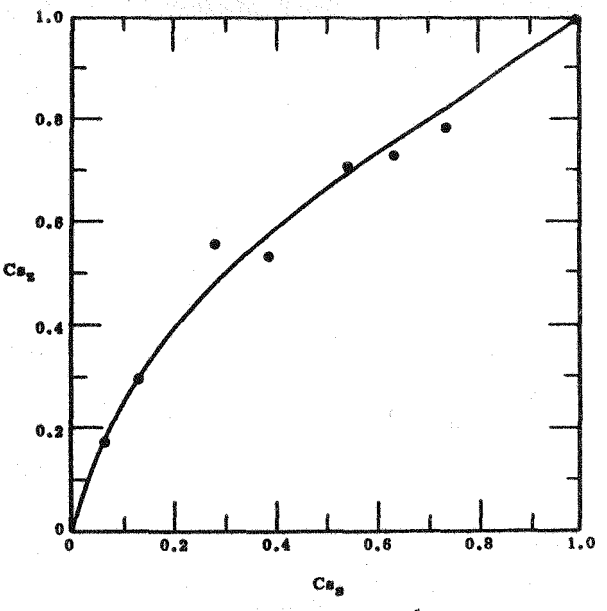

Figure 16

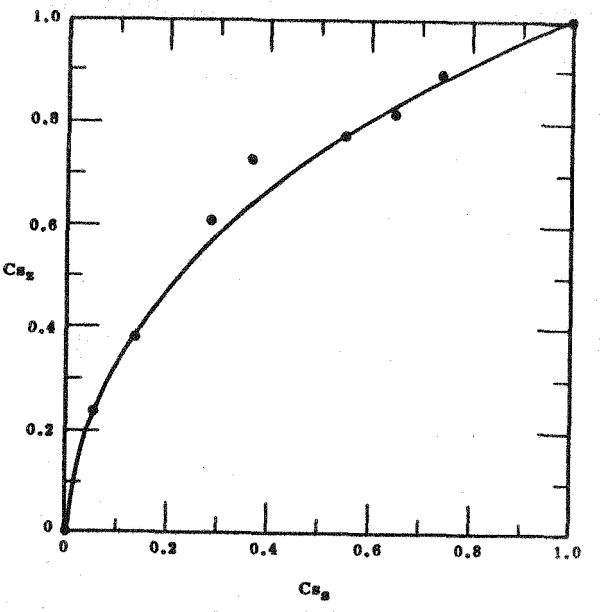

Figure 17

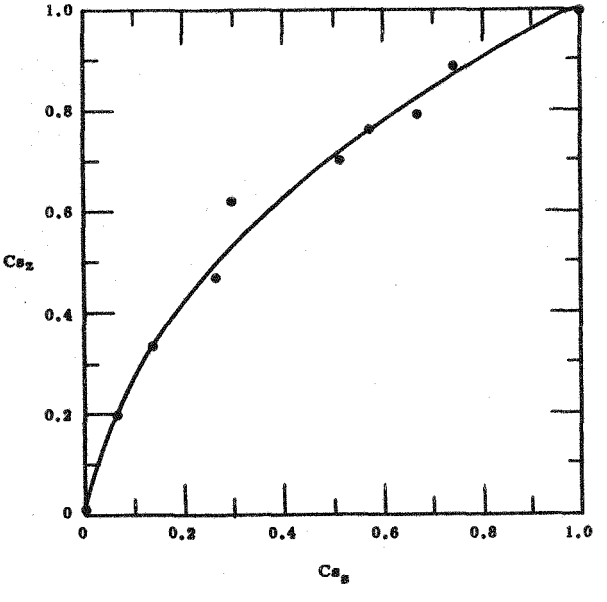

Figure 18

Figures 16, 17 and 18. The 25C isotherm for the reaction $Rb_z + Cs_s = Cs_z + Rb_s$ with AW-500, Zeolon, and clinoptilolite, respectively. Total equilibrium solution normality was constant at 0.5.

Cs_z = Equivalent fraction of cesium on the zeolite.
Cs_s = Equivalent fraction of cesium in the equilibrium solution.

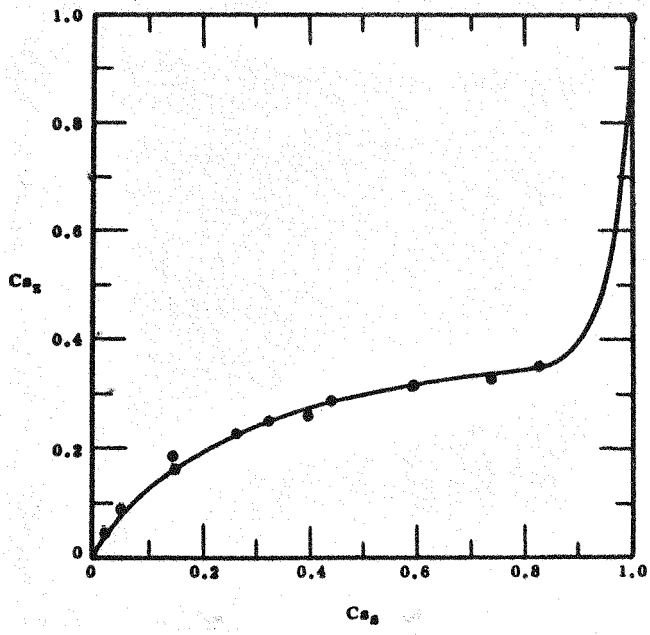

Figure 19

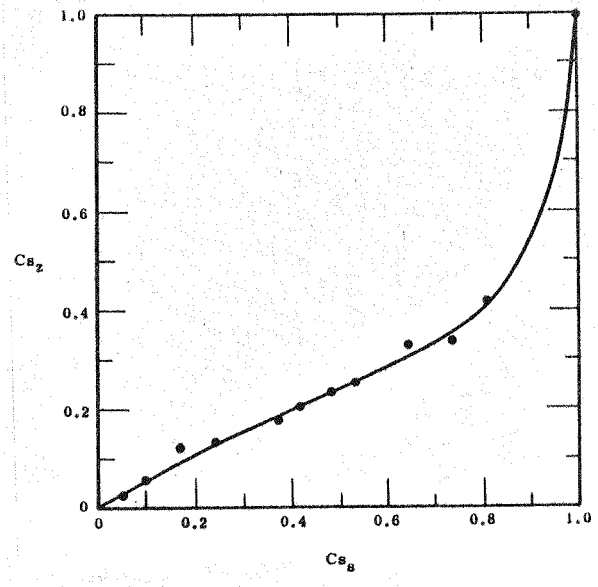

Figure 20

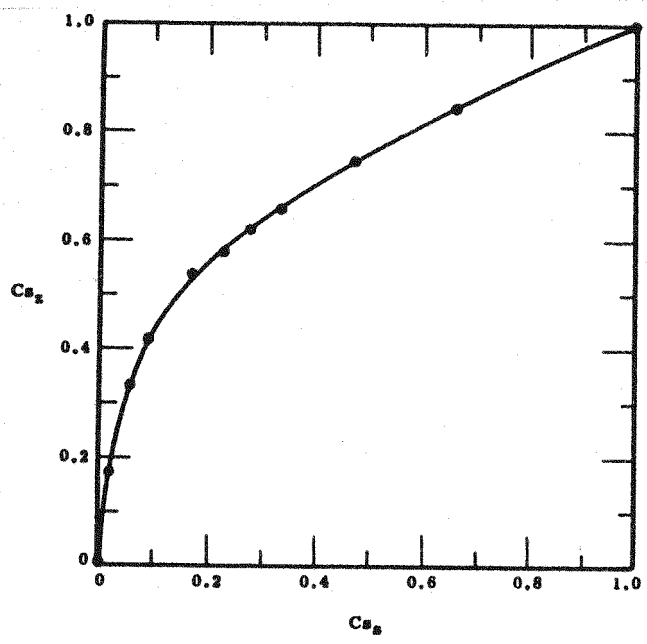

Figure 21

Figures 19, 20 and 21. The 25C isotherm for the reaction $NH_{4_Z} + Cs_S = Cs_Z + NH_{4_S}$ with 4AXW, 13X, and AW-400, respectively. Total equilibrium solution normality was constant at 0.1.

Cs_Z = Equivalent fraction of cesium on the zeolite.
Cs_S = Equivalent fraction of cesium in the equilibrium solution.

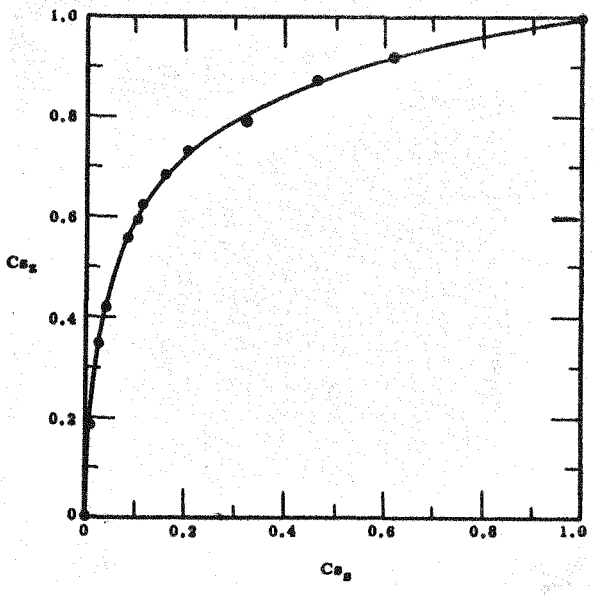

Figure 22

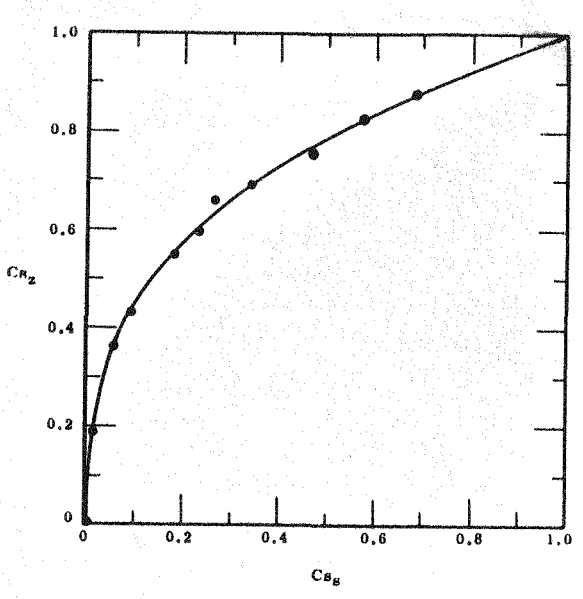

Figure 23

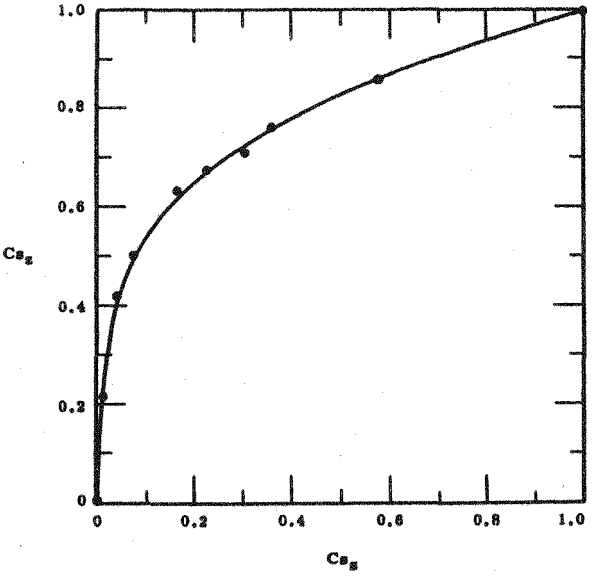

Figure 24

Figures 22, 23 and 24. The 25C isotherm for the reaction $NH_{4_Z} + Cs_S = Cs_Z + NH_{4_S}$ with AW-500, Zeolon, and clinoptilolite, respectively. Total equilibrium solution normality was constant at 0.1.

Cs_Z = Equivalent fraction of cesium on the zeolite.
Cs_S = Equivalent fraction of cesium in the equilibrium solution.

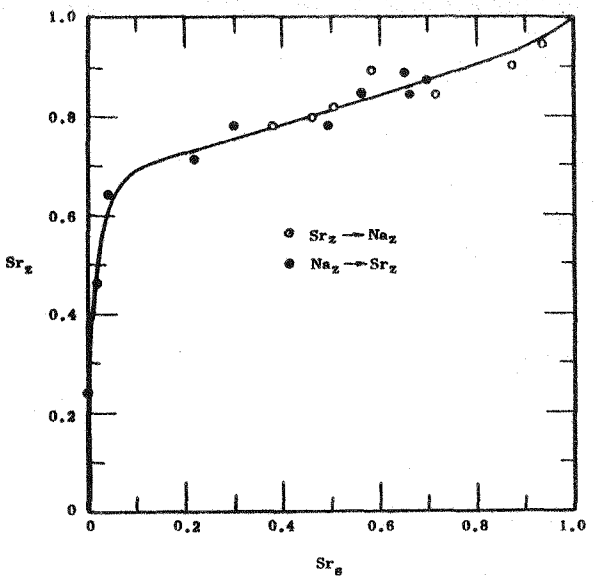

Figure 25

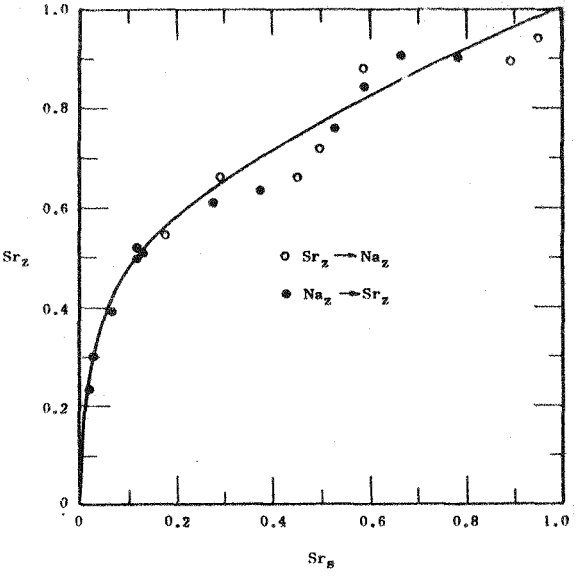

Figure 26

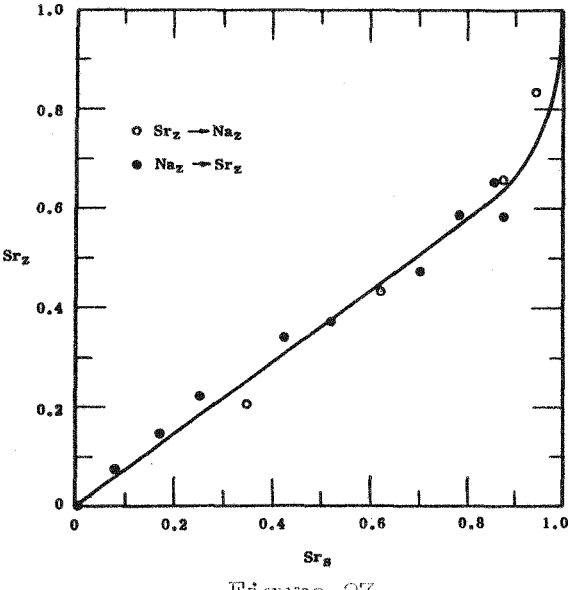

Figure 27

Figures 25, 26 and 27. The 25C isotherm for the reaction $2Na_z + Sr_s = Sr_z + 2Na_s$ with 4AXW, 13X, and AW-400, respectively. Total equilibrium solution was constant at one.

Sr_z = Equivalent fraction of strontium on the zeolite.
Sr_s = Equivalent fraction of strontium in the equilibrium solution.

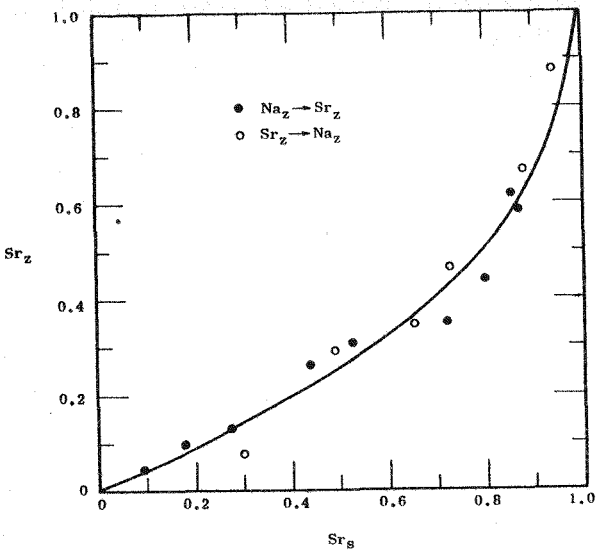

Figure 28

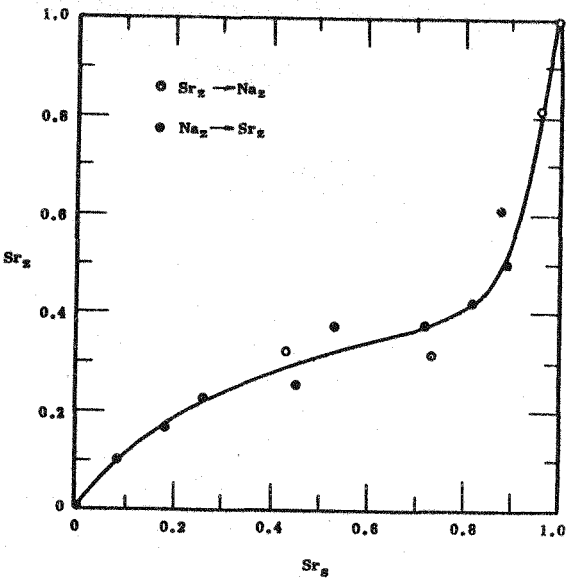

Figure 29

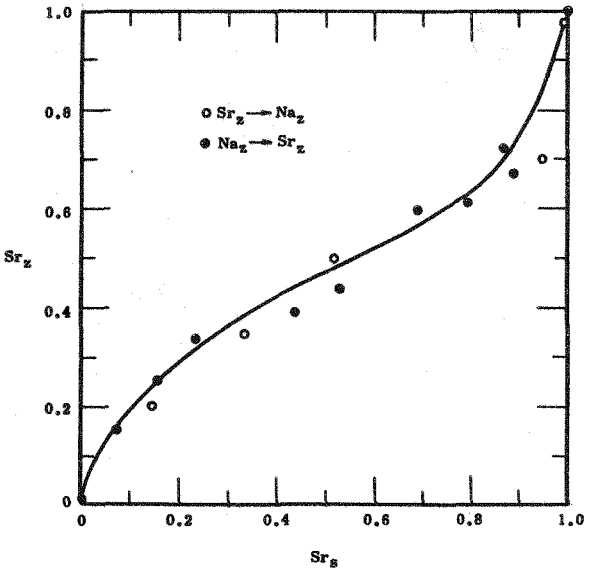

Figure 30

Figures 28, 29 and 30. The 25C isotherm for the reaction $2Na_z + Sr_s = Sr_z + 2Na_s$ with AW-500, Zeolon, and clinoptilolite, respectively. Total equilibrium solution normality was constant at one.

Sr_z = Equivalent fraction of strontium on the zeolite.
Sr_s = Equivalent fraction of strontium in the equilibrium solution.

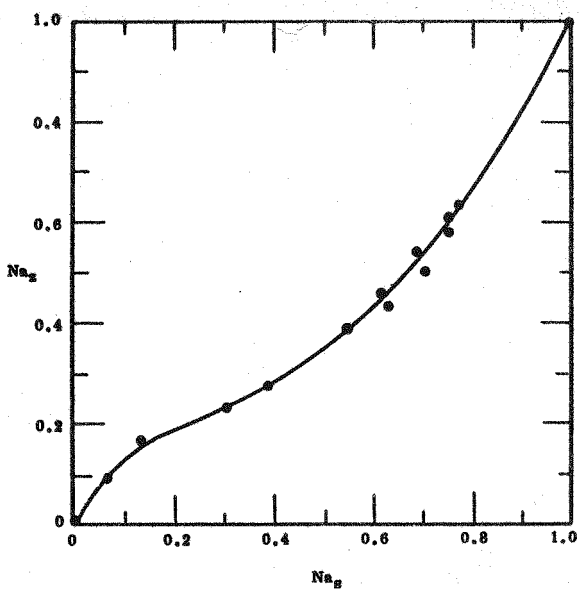

Figure 31

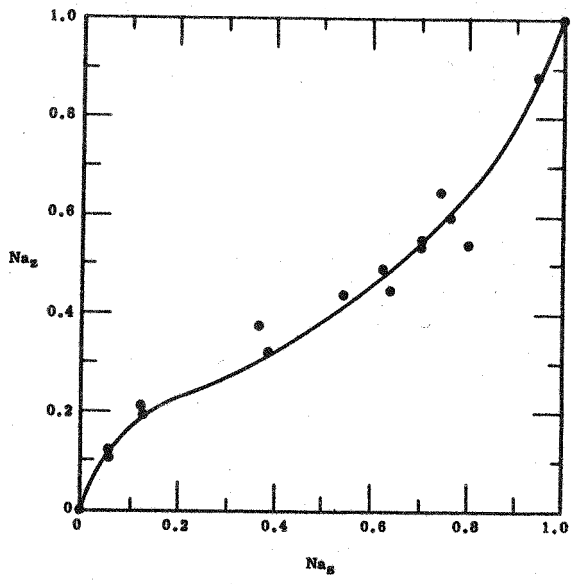

Figure 32

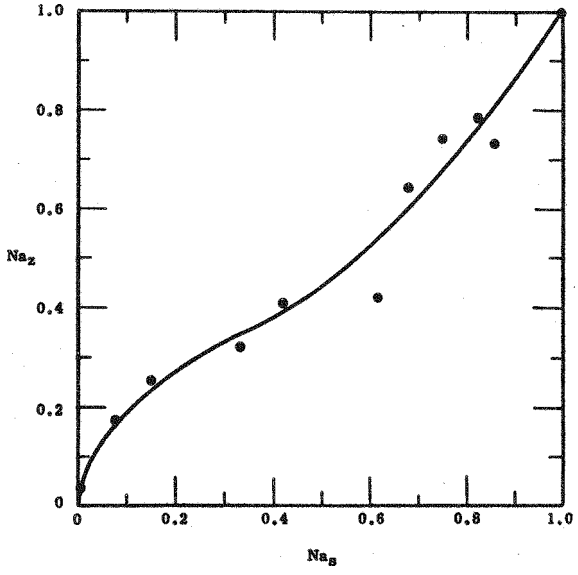

Figure 33

Figures 31, 32 and 33. The 25C isotherm for the reaction $Ca_z + 2Na_s = 2Na_z + Ca_s$ with 4AXW, 13X, and AW-400, respectively. Total equilibrium solution normality was constant at one.

Na_z = Equivalent fraction of sodium on the zeolite.
Na_s = Equivalent fraction of sodium in the equilibrium solution.

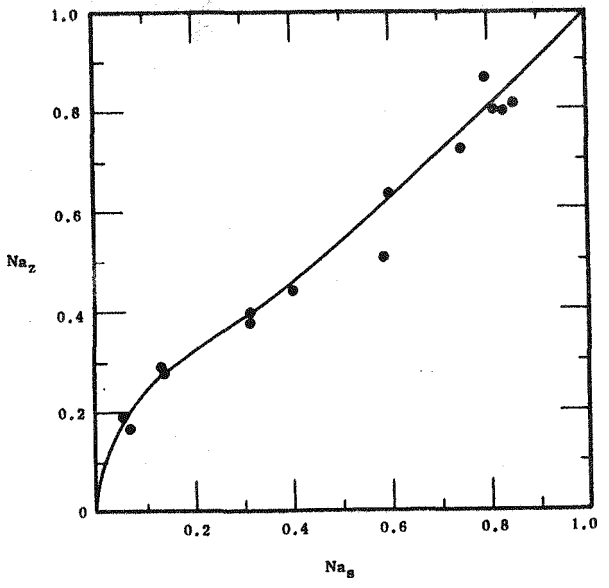

Figure 34

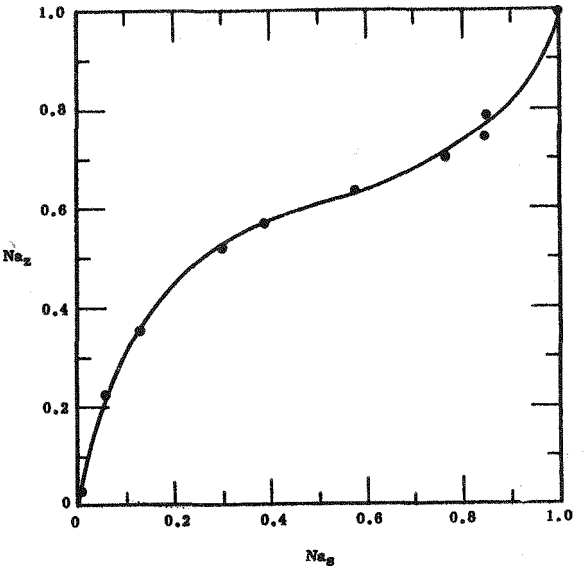

Figure 35

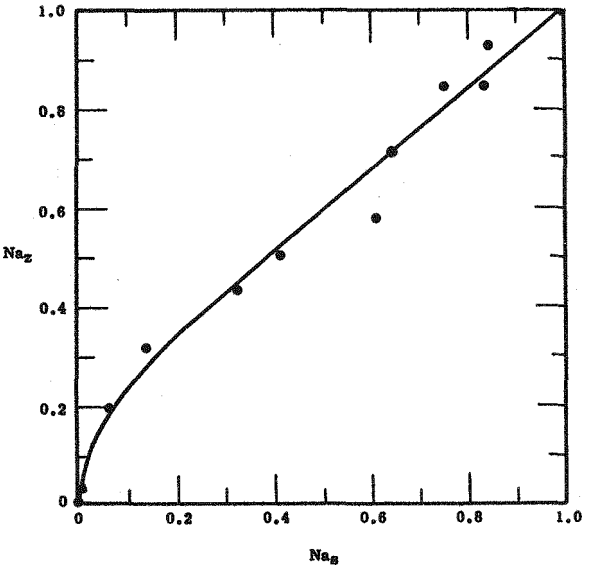

Figure 36

Figures 34, 35 and 36. The 25C isotherm for the reaction $Ca_z + 2Na_s = 2Na_z + Ca_s$ with AW-500, Zeolon, and clinoptilolite, respectively. Total equilibrium solution normality was constant at one.

Na_z = Equivalent fraction of sodium on the zeolite.
Na_s = Equivalent fraction of sodium in the equilibrium solution.

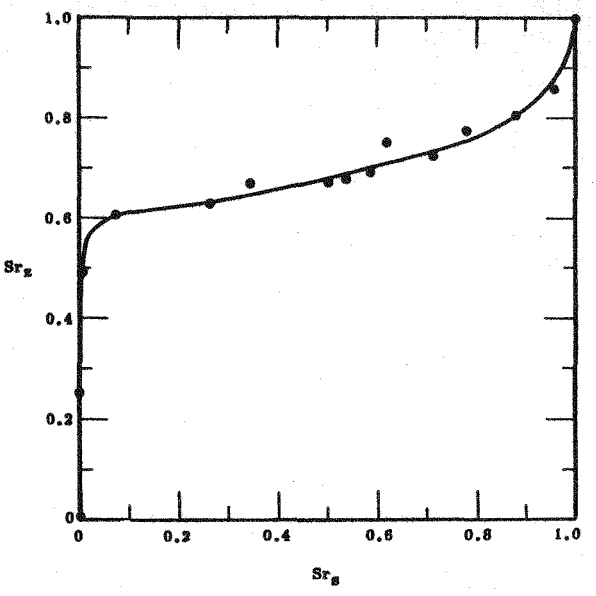

Figure 37

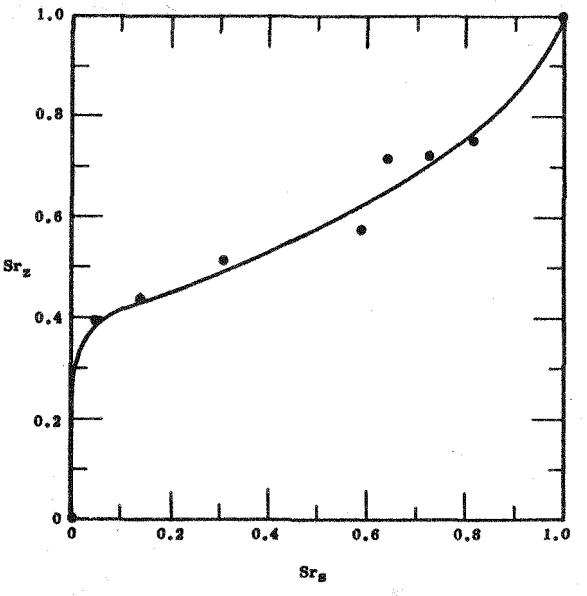

Figure 38

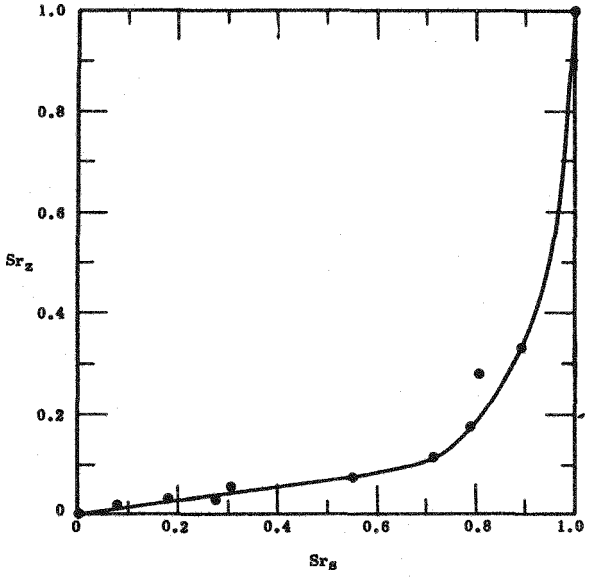

Figure 39

Figures 37, 38 and 39. The 25C isotherm for the reaction $2Cs_Z + Sr_S = Sr_Z + 2Cs_S$ with 4AXW, 13X, and AW-400, respectively. Total equilibrium solution normality was constant at one.

Sr_Z = Equivalent fraction of strontium on the zeolite.
Sr_S = Equivalent fraction of strontium in the equilibrium solution.

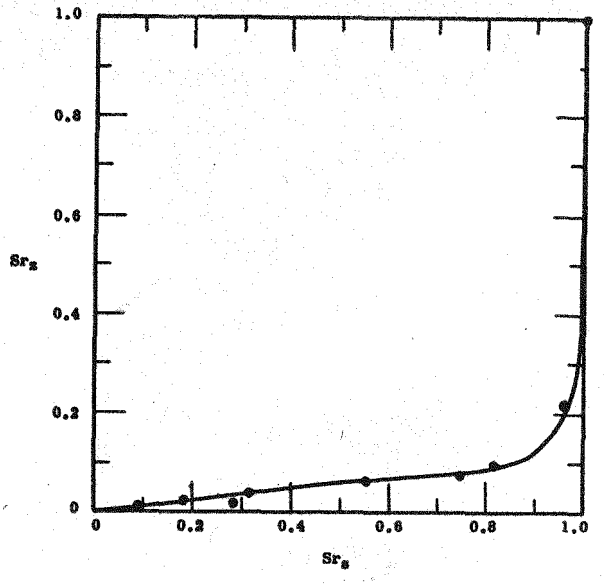

Figure 40

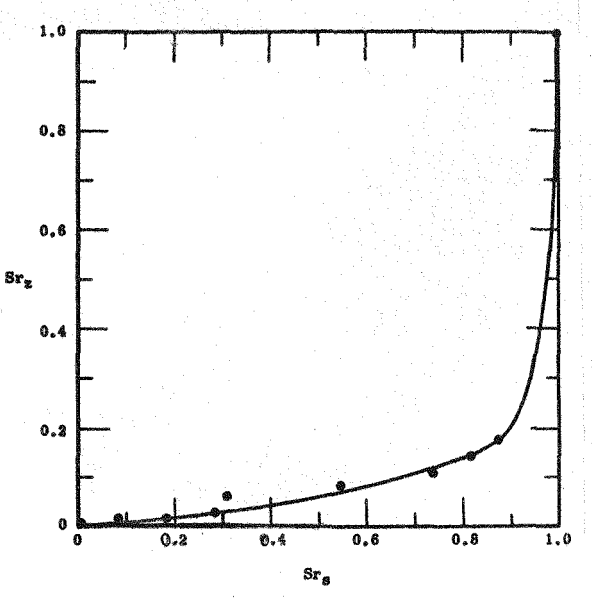

Figure 41

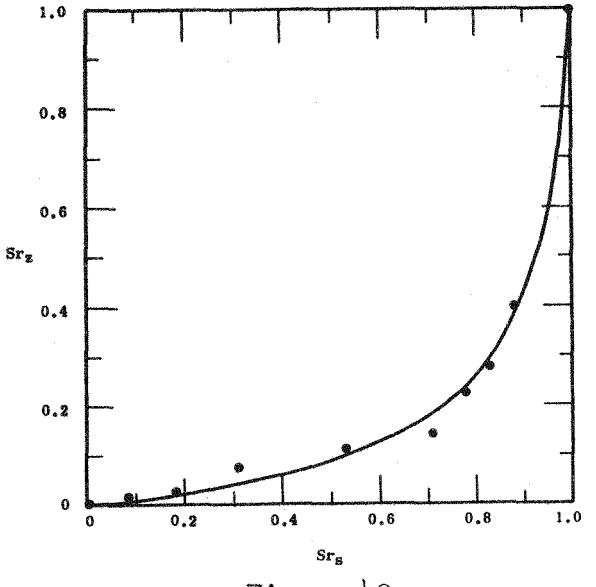

Figure 42

Figures 40, 41 and 42. The 25C isotherm for the reaction $2Cs_z + Sr_s = Sr_z + 2Cs_s$ with AW-500, Zeolon, and clinoptilolite, respectively. Total equilibrium solution normality was constant at one.

Sr_z = Equivalent fraction of strontium on the zeolite.
Sr_s = Equivalent fraction of strontium in the equilibrium solution.

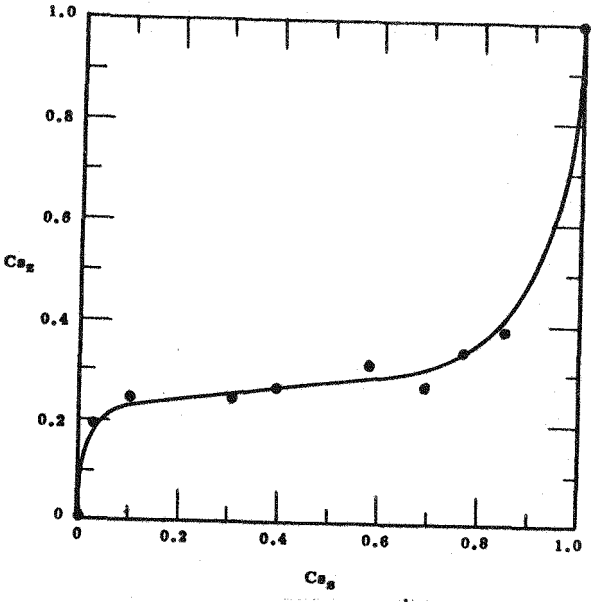

Figure 43

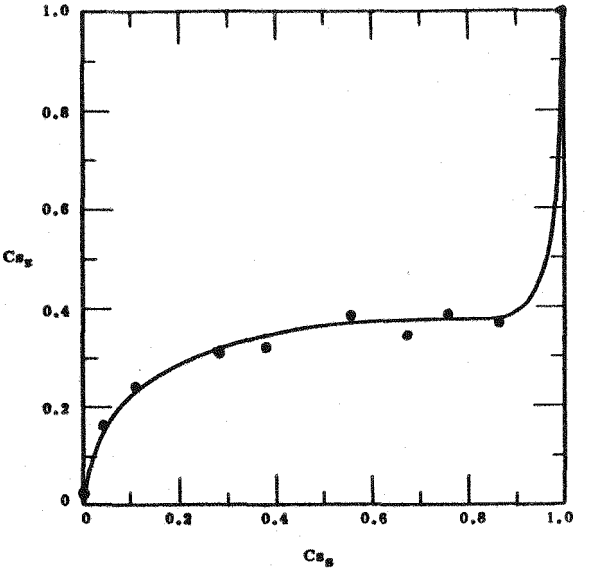

Figure 44

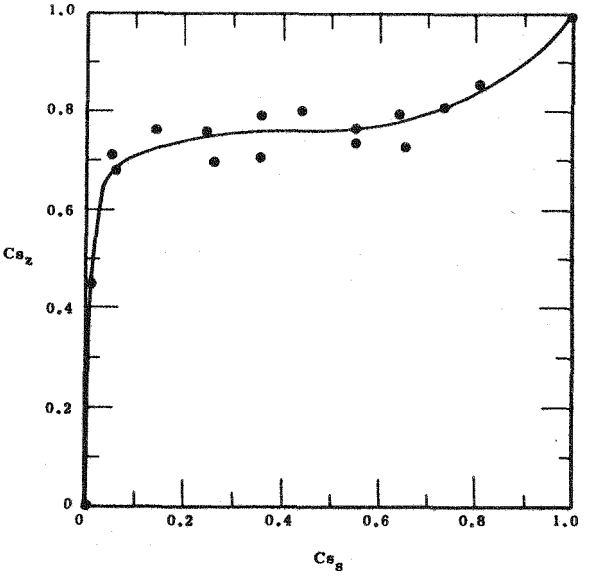

Figure 45

Figures 43, 44 and 45. The 25C isotherm for the reaction $Ca_z + 2Cs_s = 2Cs_z + Ca_s$ with 4AXW, 13X, and AW-400, respectively. Total equilibrium solution normality was constant at one.

Cs_z = Equivalent fraction of cesium on the zeolite.
Cs_s = Equivalent fraction of cesium in the equilibrium solution.

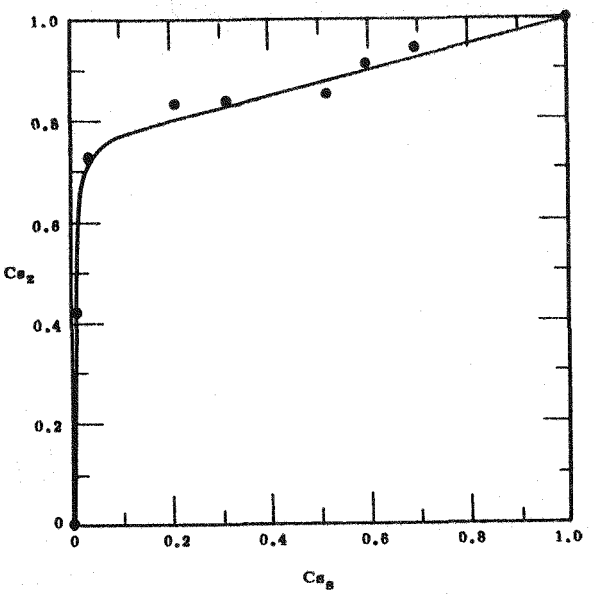

Figure 46

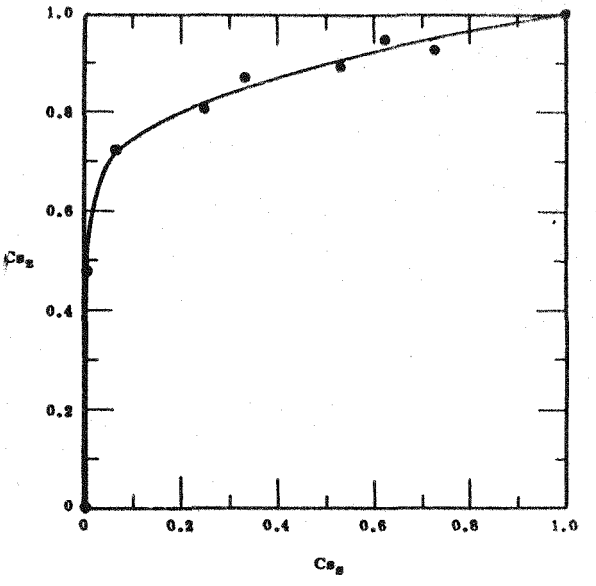

Figure 47

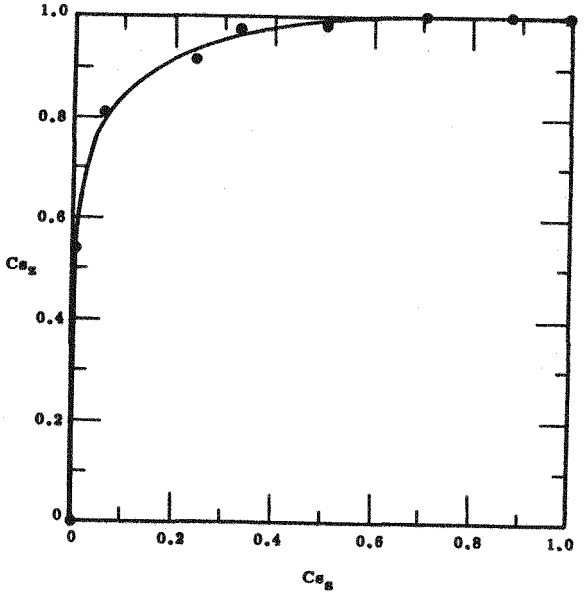

Figure 48

Figures 46, 47 and 48. The 25C isotherm for the reaction $Ca_z + 2Cs_s = 2Cs_z + Ca_s$ with AW-500, Zeolon, and clinoptilolite, respectively. Total equilibrium solution normality was constant at one.

Cs_z = Equivalent fraction of cesium on the zeolite.
Cs_s = Equivalent fraction of cesium in the equilibrium solution.

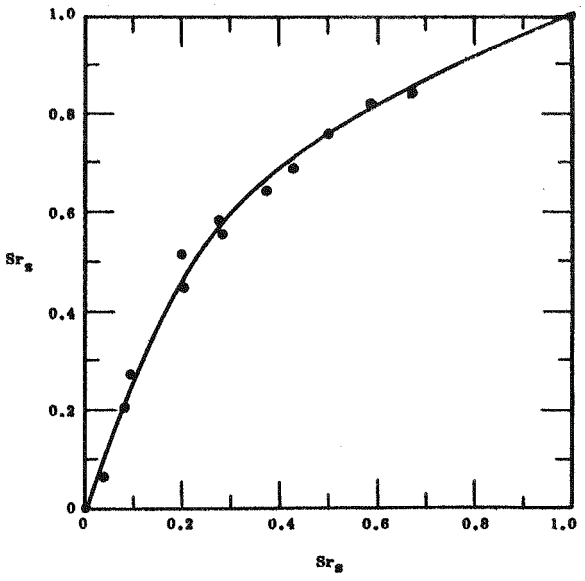

Figure 49

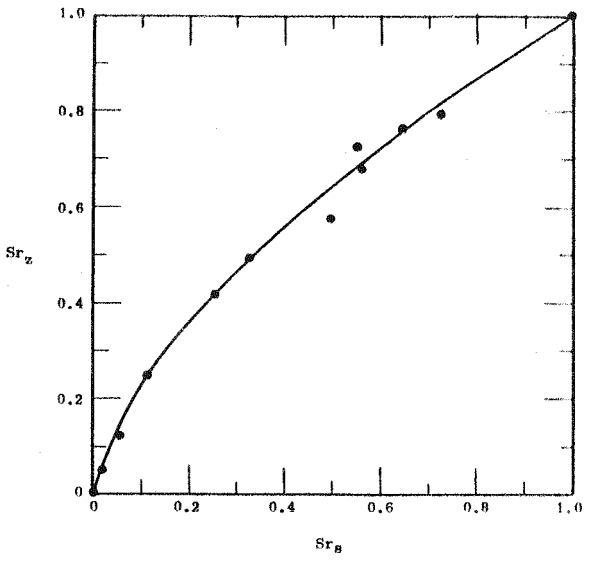

Figure 50

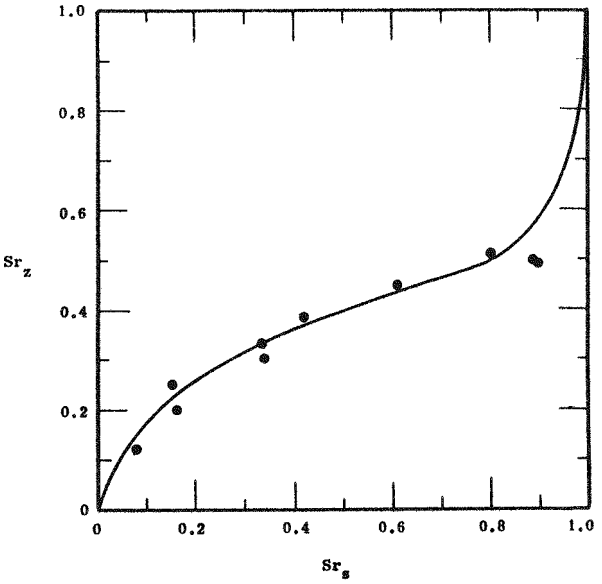

Figure 51

Figures 49, 50 and 51. The 25C isotherm for the reaction $Ca_z + Sr_s = Sr_z + Ca_s$ with 4AXW, 13X, and AW-400, respectively. Total equilibrium solution normality was constant at one.

Sr_z = Equivalent fraction of strontium on the zeolite.
Sr_s = Equivalent fraction of strontium in the equilibrium solution.

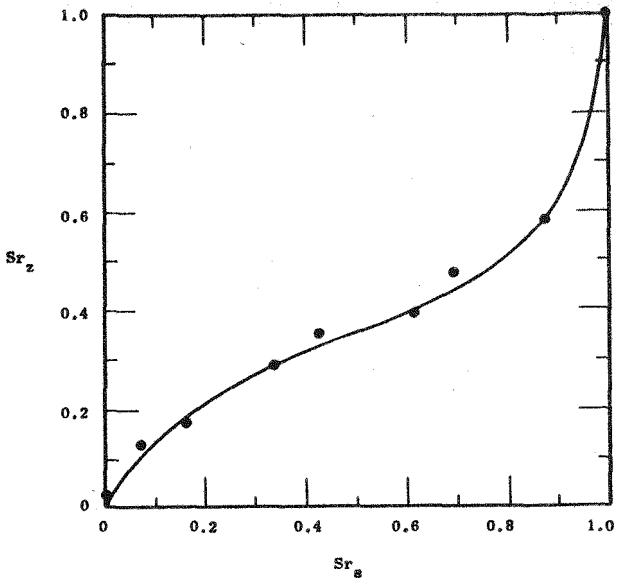

Figure 52

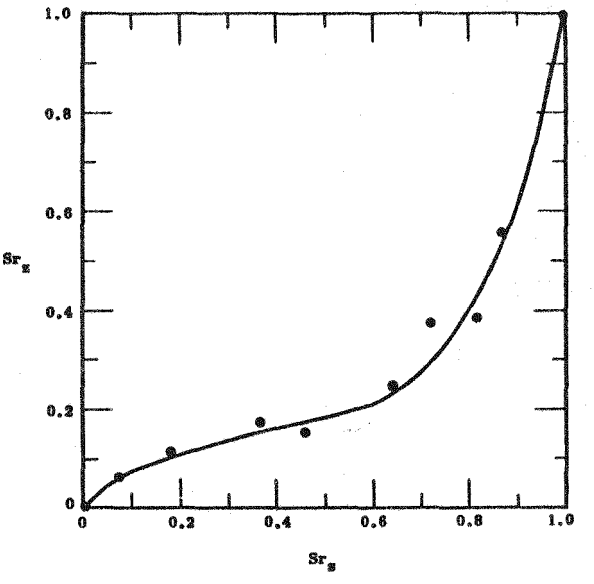

Figure 53

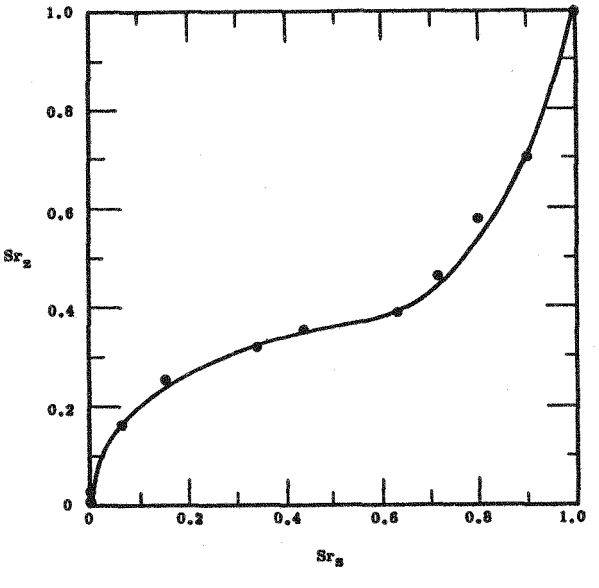

Figure 54

Figures 52, 53 and 54. The 25C isotherm for the reaction $Ca_z + Sr_s = Sr_z + Ca_s$ with AW-500, Zeolon, and clinoptilolite, respectively. Total equilibrium solution normality was constant at one.

Sr_z = Equivalent fraction of strontium on the zeolite.
Sr_s = Equivalent fraction of strontium in the equilibrium solution.

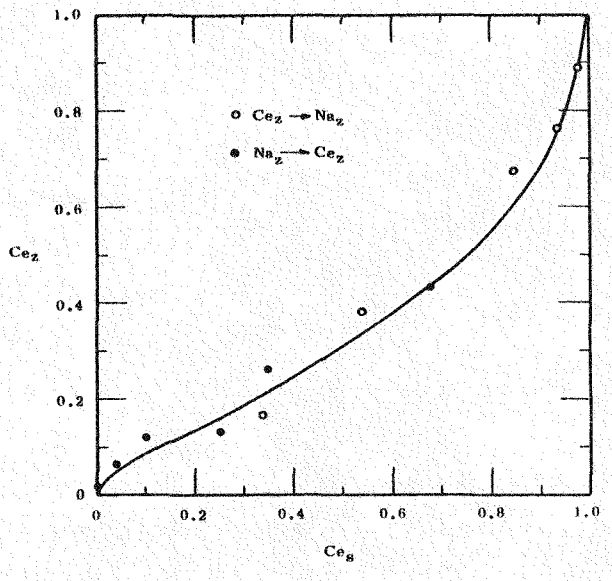

Figure 55

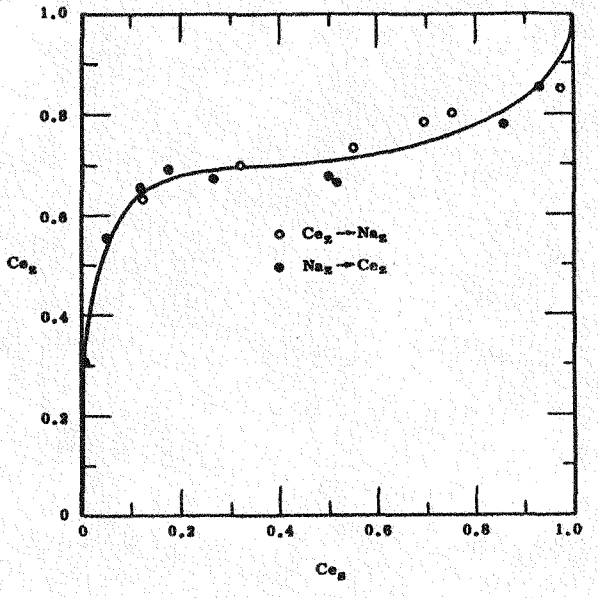

Figure 56

Figures 55 and 56. The 25C isotherm for the reaction $3Na_Z + Ce_S = Ce_Z + 3Na_S$ with 4AXW, and 13X, respectively. Total equilibrium solution normality was constant at 0.5.

Ce_Z = Equivalent fraction of cerium on the zeolite.
Ce_S = Equivalent fraction of cerium in the equilibrium solution.

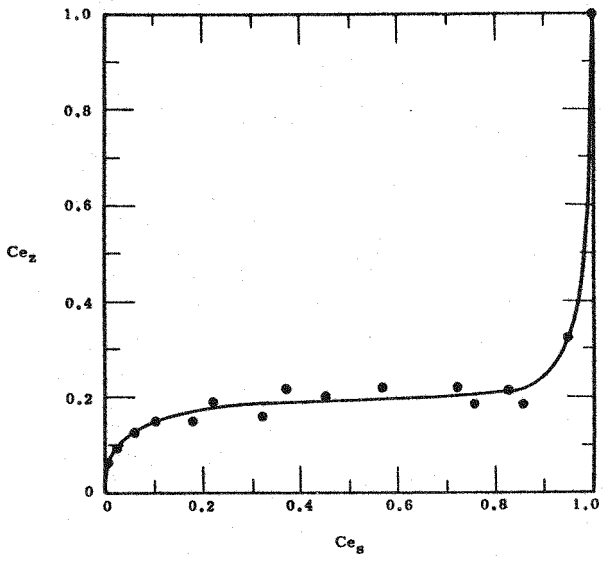

Figure 57

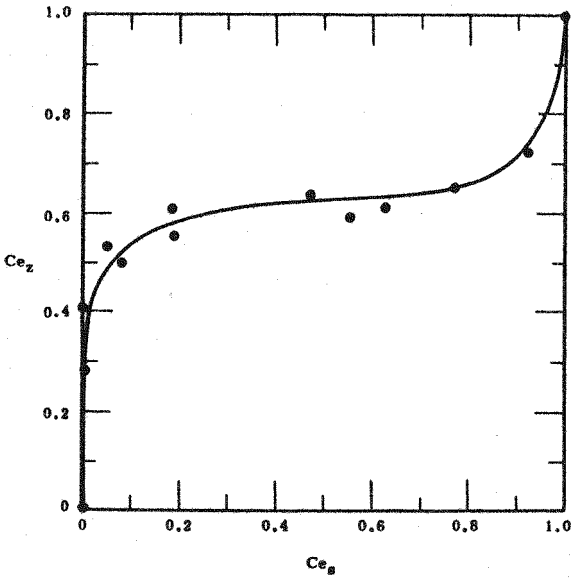

Figure 58

Figures 57 and 58. The 25C isotherm for the reaction $3Cs_z + Ce_s = Ce_z + 3Cs_s$ with 4AXW, and 13X, respectively. Total equilibrium solution normality was constant at 0.5.

Ce_z = Equivalent fraction of cerium on the zeolite.
Ce_s = Equivalent fraction of cerium in the equilibrium solution.

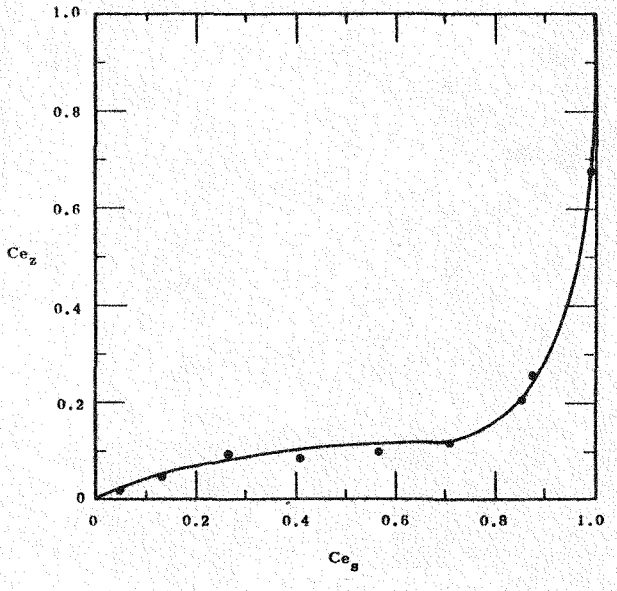

Figure 59

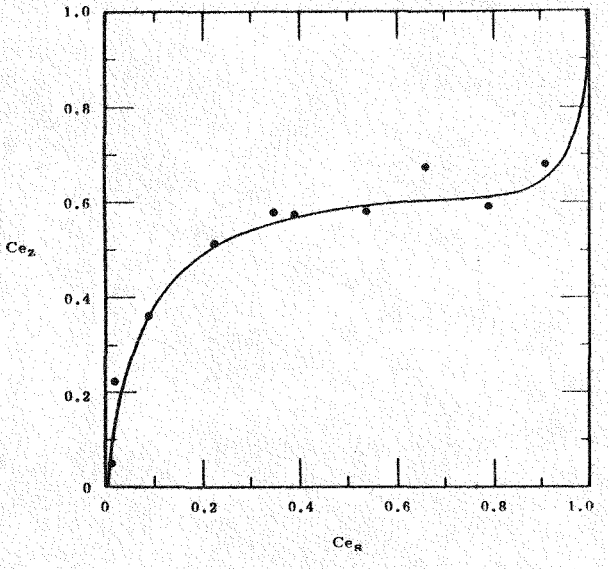

Figure 60

Figures 59 and 60. The 25C isotherm for the reaction $3Sr_z + 2Ce_s = 2Ce_z + 3Sr_s$ with 4AXW, and 13X, respectively. Total equilibrium solution normality was constant at 0.5.

Ce_z = Equivalent fraction of cerium on the zeolite.
Ce_s = Equivalent fraction of cerium in the equilibrium solution.

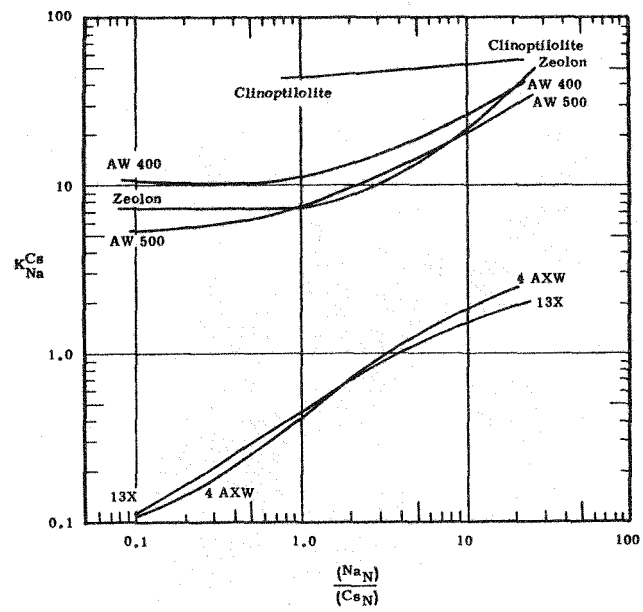

Figure 61. Variation of mass action quotients with solution equivalent ratios for the exchange reaction $Na_{zeolite} + Cs_{solution} = Cs_{zeolite} + Na_{solution}$.

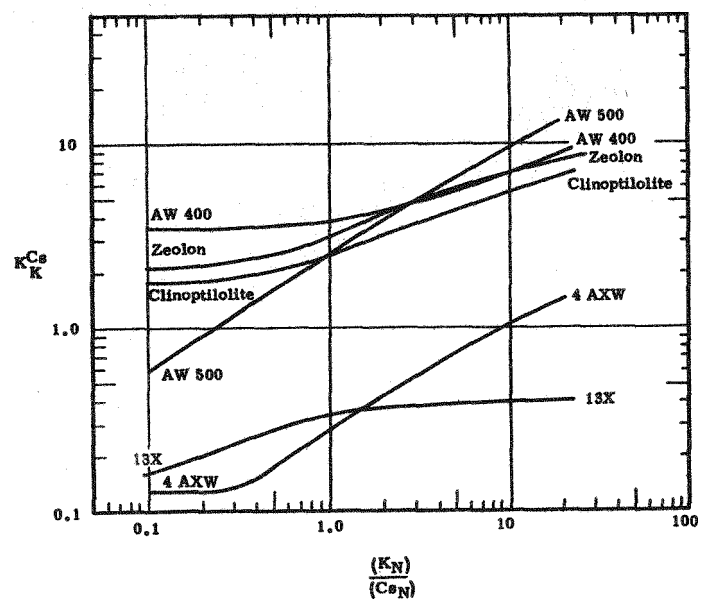

Figure 62. Variation of mass action quotients with solution equivalent ratios for the reaction $K_{zeolite} + Cs_{solution} = Cs_{zeolite} + K_{solution}$.

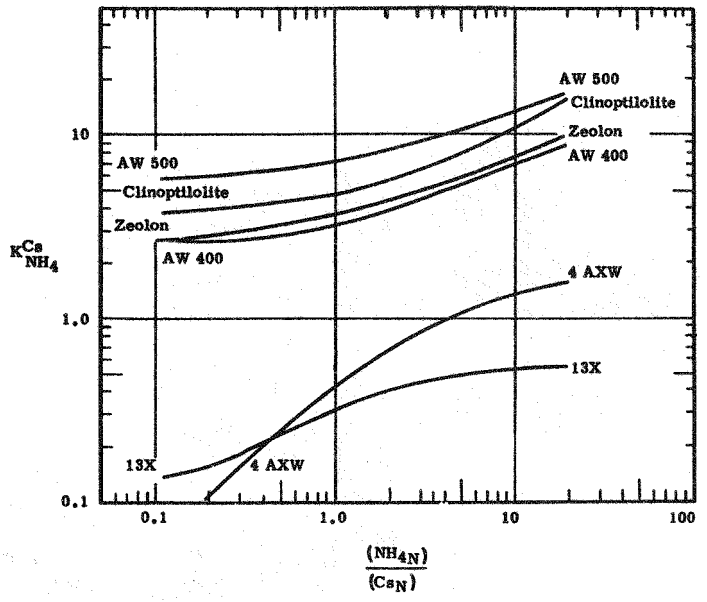

Figure 63. Variation of mass action quotients with solution equivalent ratios for the exchange reaction NH_4 zeolite + Cs solution = Cs zeolite + NH_4 solution.

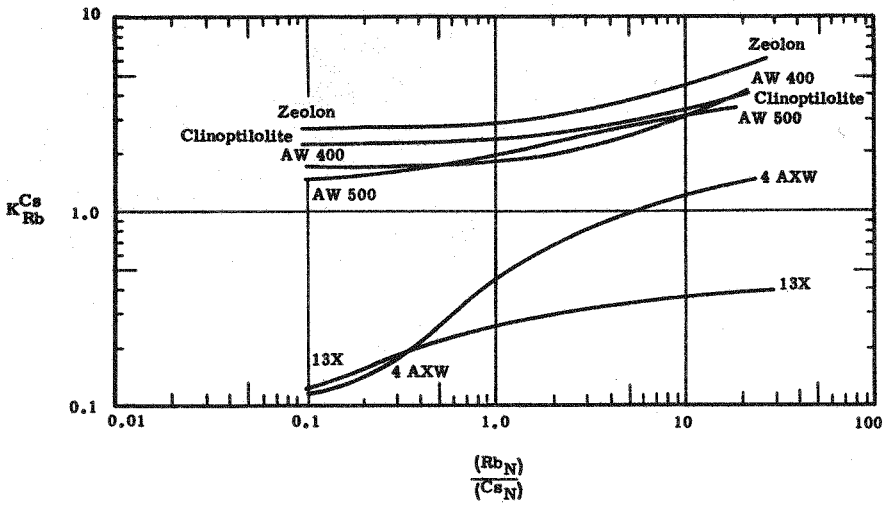

Figure 64. Variation of mass action quotients with solution equivalent ratios for the exchange reaction $Rb_{zeolite} + Cs_{solution} = Cs_{zeolite} + Rb_{solution}$.

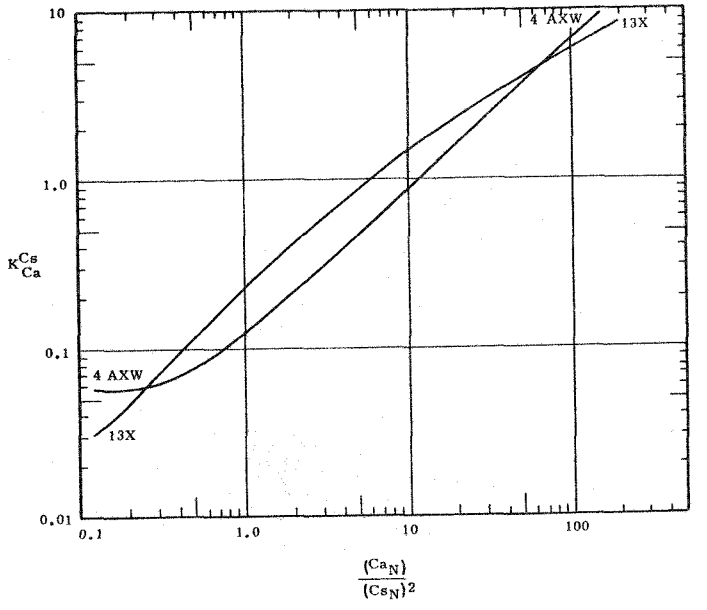

Figure 65. Variation of mass action quotient with solution equivalent ratios for the exchange reaction $Ca_{zeolite} + 2Cs_{solution} = 2Cs_{zeolite} + Ca_{solution}$.

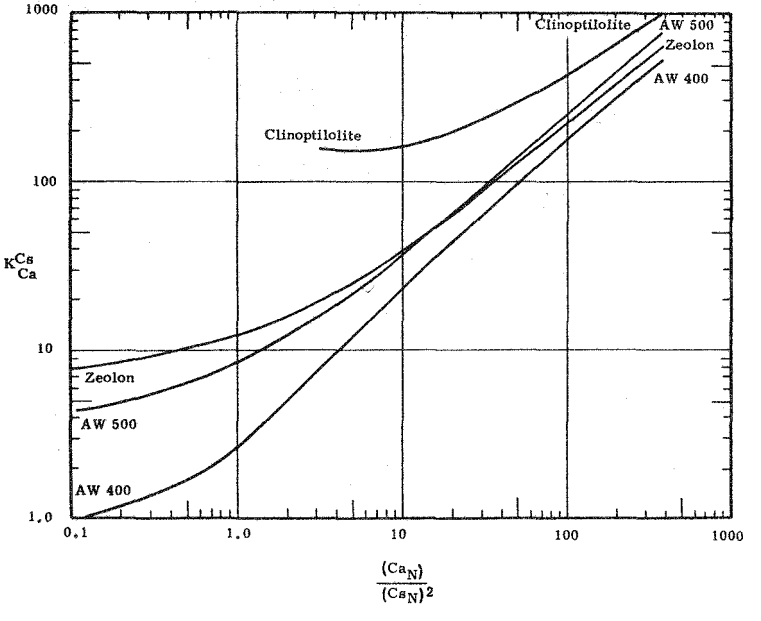

Figure 66. Variation of mass action quotients with solution equivalent ratios for the exchange reaction $Ca_{zeolite} + 2Cs_{solution} = 2Cs_{zeolite} + Ca_{solution}$.

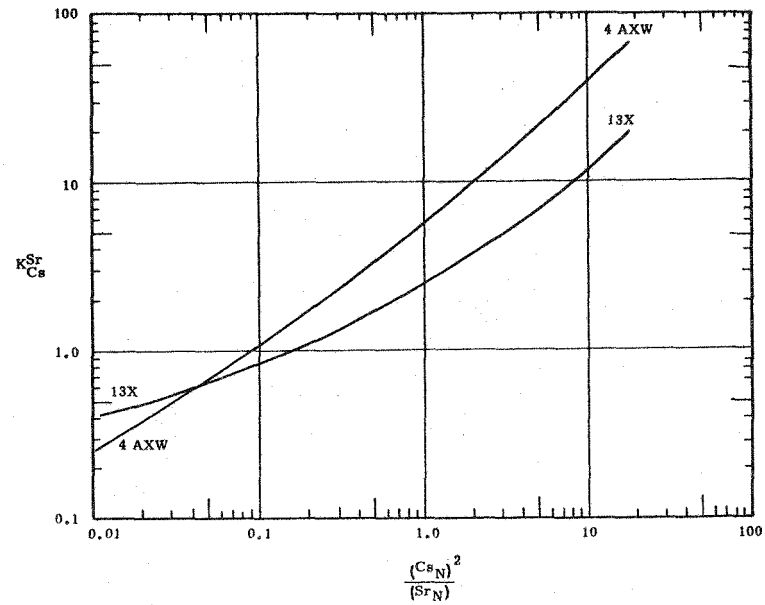

Figure 67. Variation of mass action quotients with solution equivalent ratios for the exchange reaction $2Cs_{zeolite} + Sr_{solution} = Sr_{zeolite} + 2Cs_{solution}$.

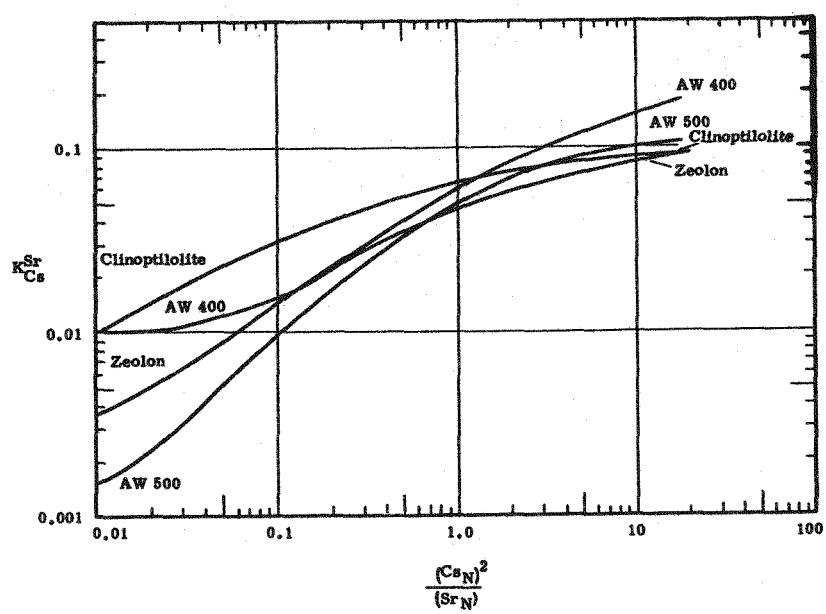

Figure 68. Variation of mass action quotients with solution equivalent ratios for the exchange reaction $2Cs_{zeolite} + Sr_{solution} = Sr_{zeolite} + 2Cs_{solution}$.

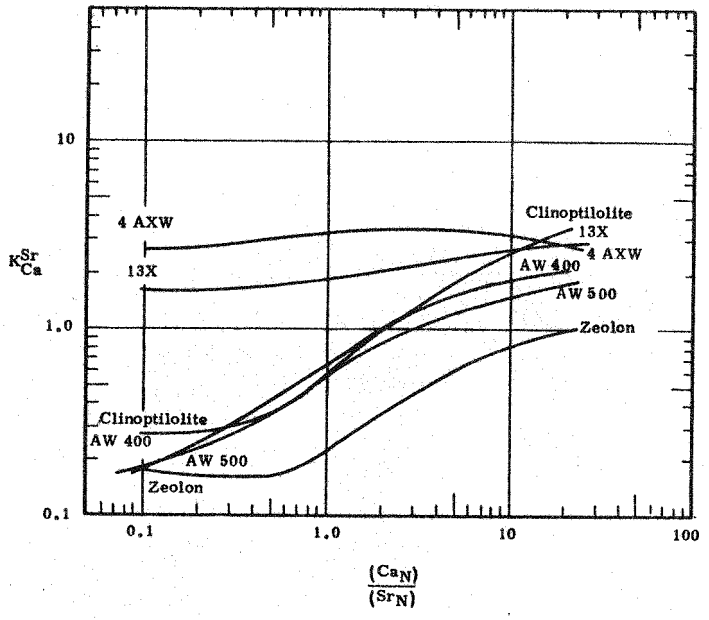

Figure 69. Variation of mass action quotients with solution equivalent ratios for the exchange reaction $Ca_{zeolite} + Sr_{solution} = Sr_{zeolite} + Ca_{solution}$.

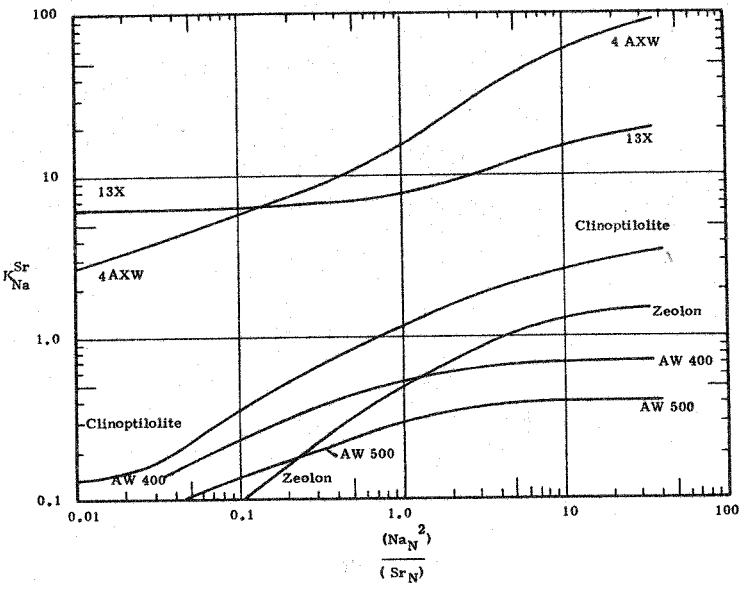

Figure 70. Variation of mass action quotients with solution equivalent ratios for the exchange reaction $2Na_{zeolite} + Sr_{solution} = Sr_{zeolite} + 2Na_{solution}$.

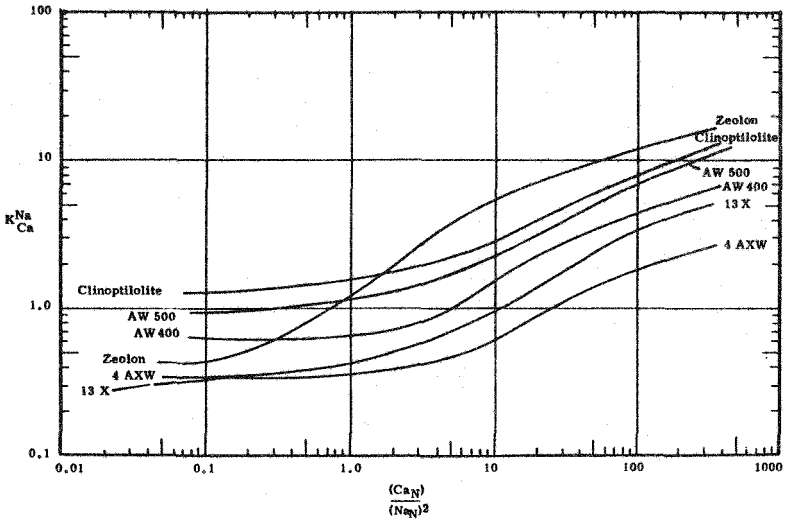

Figure 71. Variation of mass action quotients with solution equivalent ratios for the exchange reaction $Ca_{zeolite} + 2Na_{solution} = 2Na_{zeolite} + Ca_{solution}$.

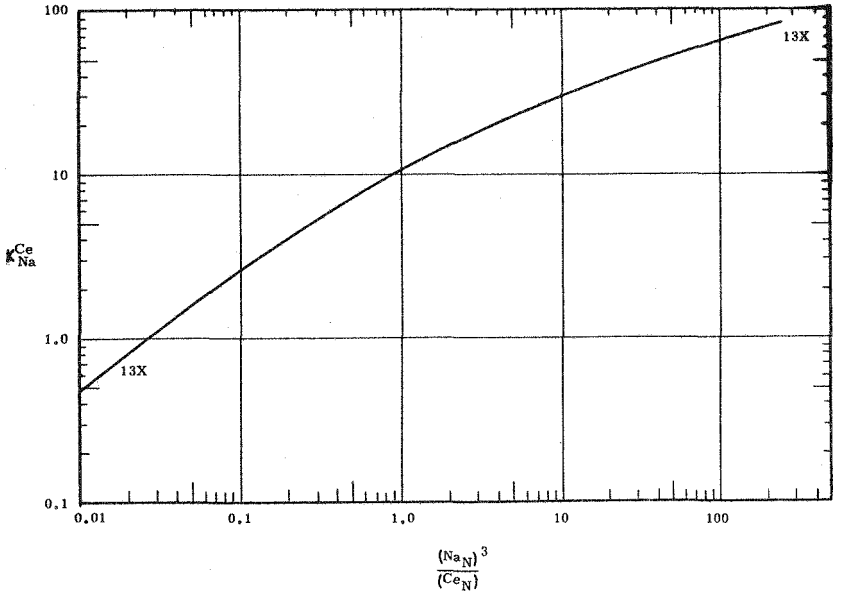

Figure 72. Variation of mass action quotients with solution equivalent ratios for the exchange reaction $3Na_{zeolite} + Ce_{solution} = Ce_{zeolite} + 3Na_{solution}$.

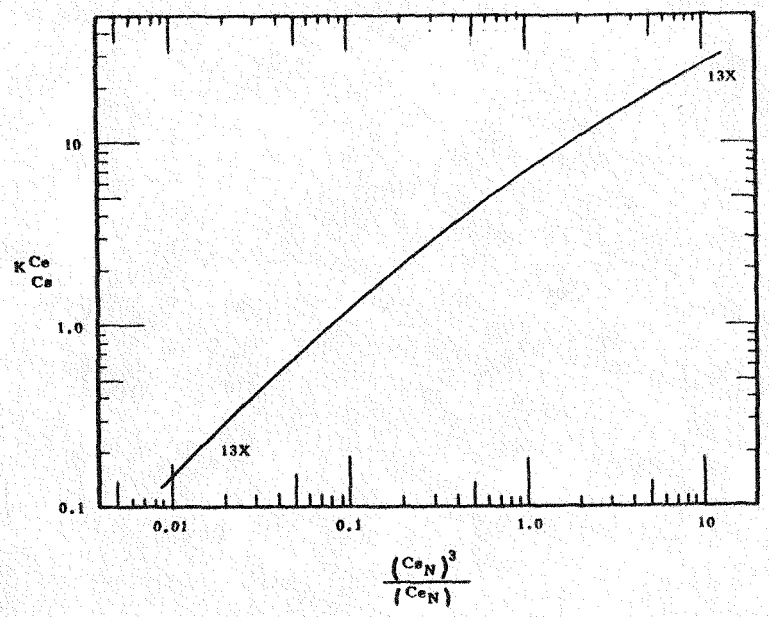

Figure 73. Variation of mass action quotients with solution equivalent ratios for the exchange reaction $3Cs_{zeolite} + Ce_{solution} = Ce_{zeolite} + 3Cs_{solution}$.

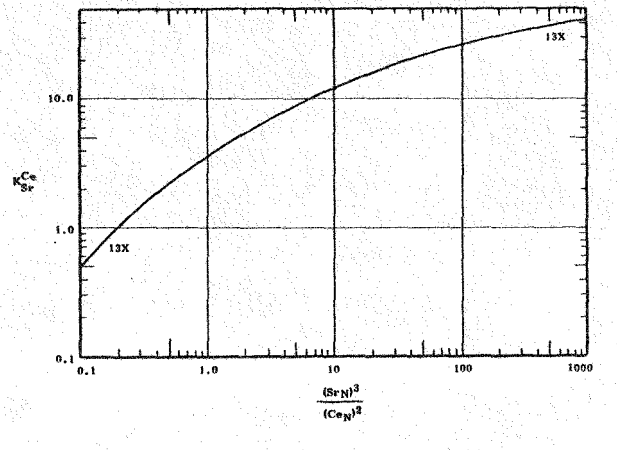

Figure 74. Variation of mass action quotients with solution equivalent ratios for the exchange reaction $3Sr_{zeolite} + 2Ce_{solution} = 2Ce_{zeolite} + 3Sr_{solution}$.

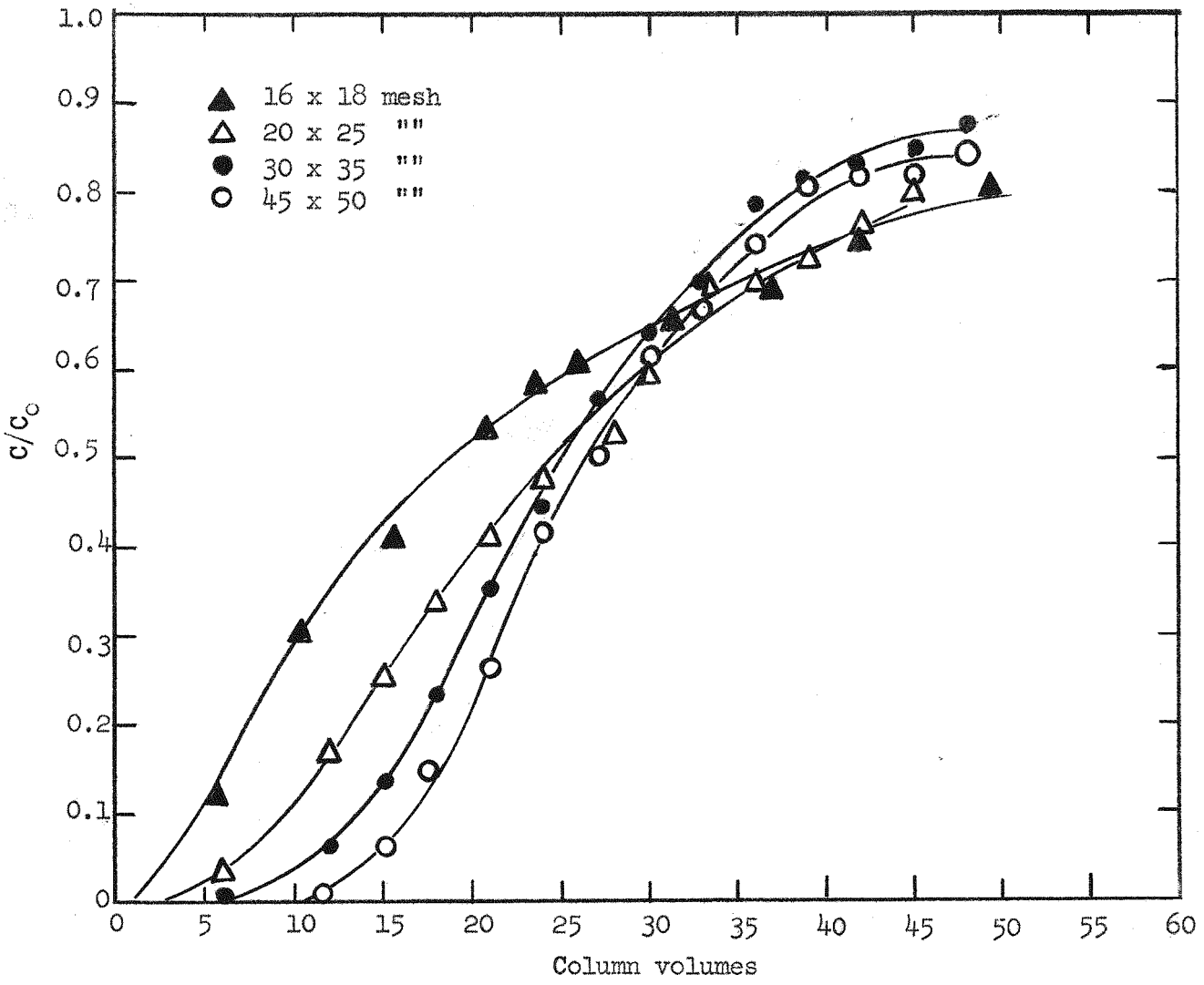

Figure 75. Effect of particle size on strontium breakthrough curves with 4A at 25C.

Conditions:

Feed	0.20M $NaNO_3$, 0.035M $Sr(NO_3)_2$, 0.010M $Ca(NO_3)_2$.
Column size	1.9 cm. diameter, 21 cm. height
Exchanger weight	50 grams
Flow rate	12 c.v./hour

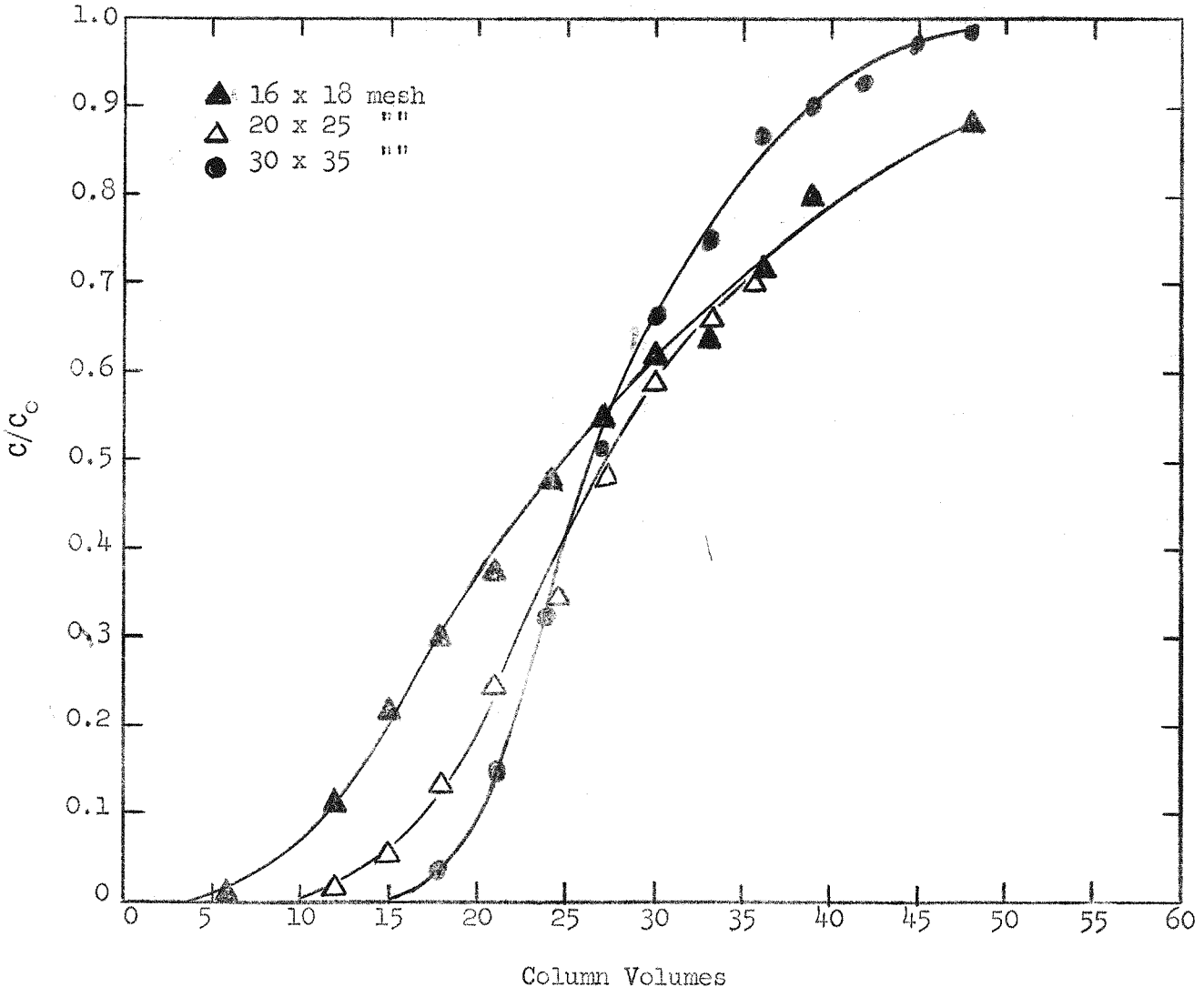

Figure 76. Effect of particle size on strontium breakthrough curve with 4A at 55C.

Conditions:

Feed	0.20M, $NaNO_3$, 0.035M $Sr(NO_3)_2$, 0.010M $Ca(NO_3)_2$.
Column size	1.9 cm. diameter, 21 cm. height
Exchanger weight	50 grams
Flow rate	12 c.v./hour

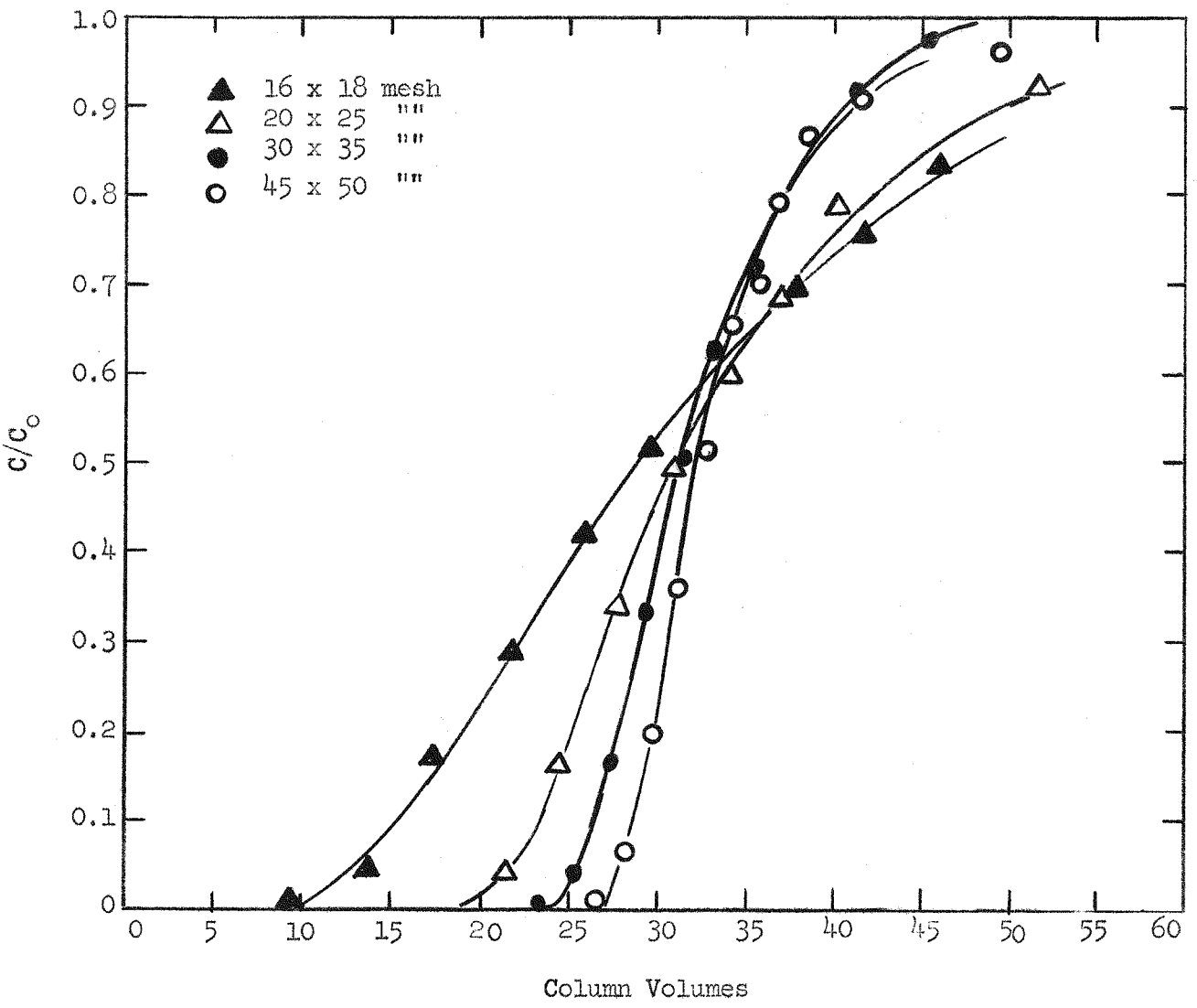

Figure 77. Effect of particle size on strontium breakthrough curve with 4A zeolite at 80C.

Conditions:

Feed	0.20M $NaNO_3$, 0.035M $Sr(NO_3)_2$, 0.010M $Ca(NO_3)_2$.
Column size	1.9 cm. diameter, 21 cm. height
Exchanger weight	50 grams
Flow rate	12 c.v./hour

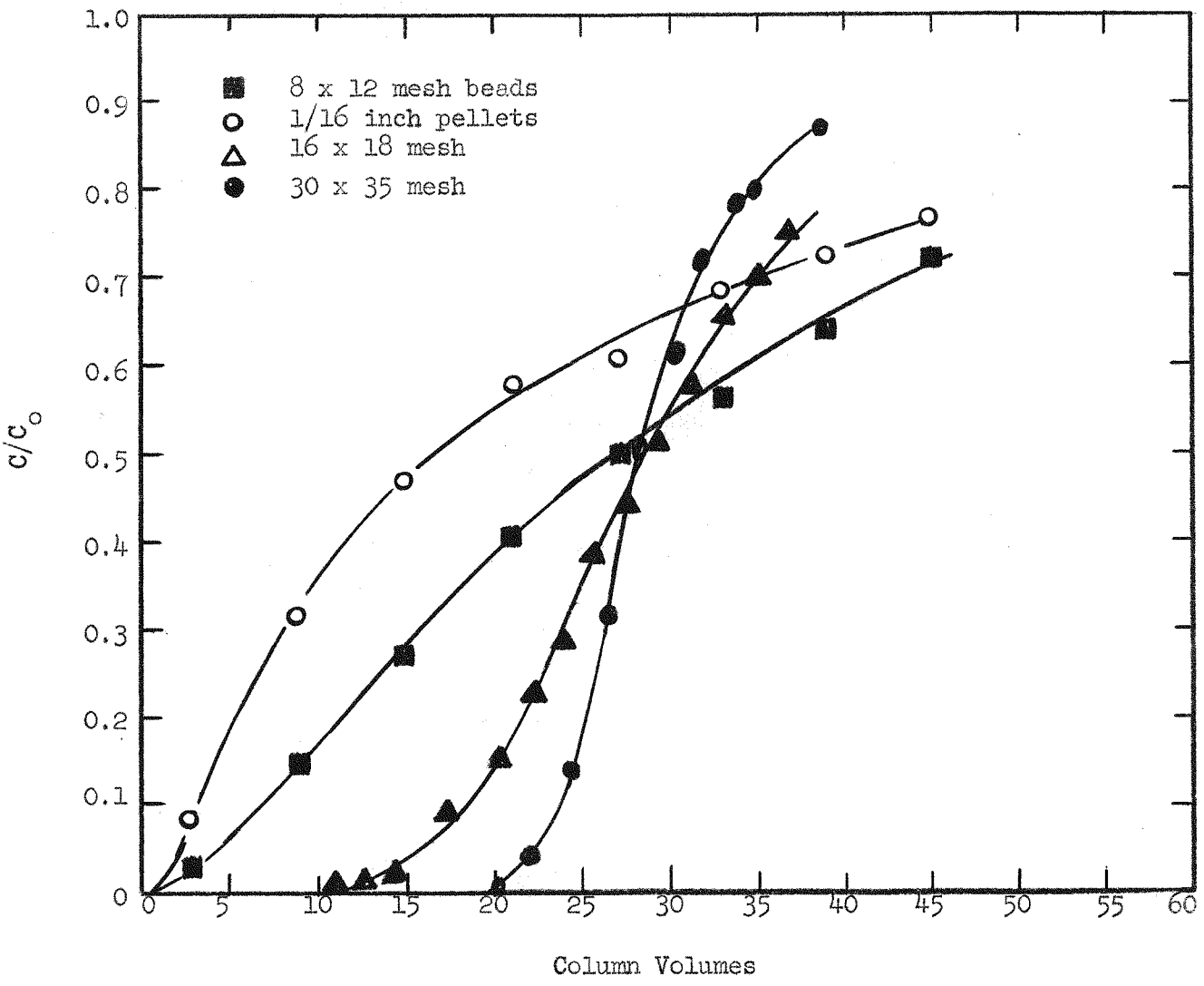

Figure 78. Effect of particle size on the strontium breakthrough curves with 4A at 25C.

Conditions:

Feed	0.20M $NaNO_3$, 0.035M $Sr(NO_3)_2$, 0.010M $Ca(NO_3)_2$.
Column size	1.9 cm. diameter, 21 cm. height
Exchanger weight	50 grams
Flow rate	3 c.v./hour

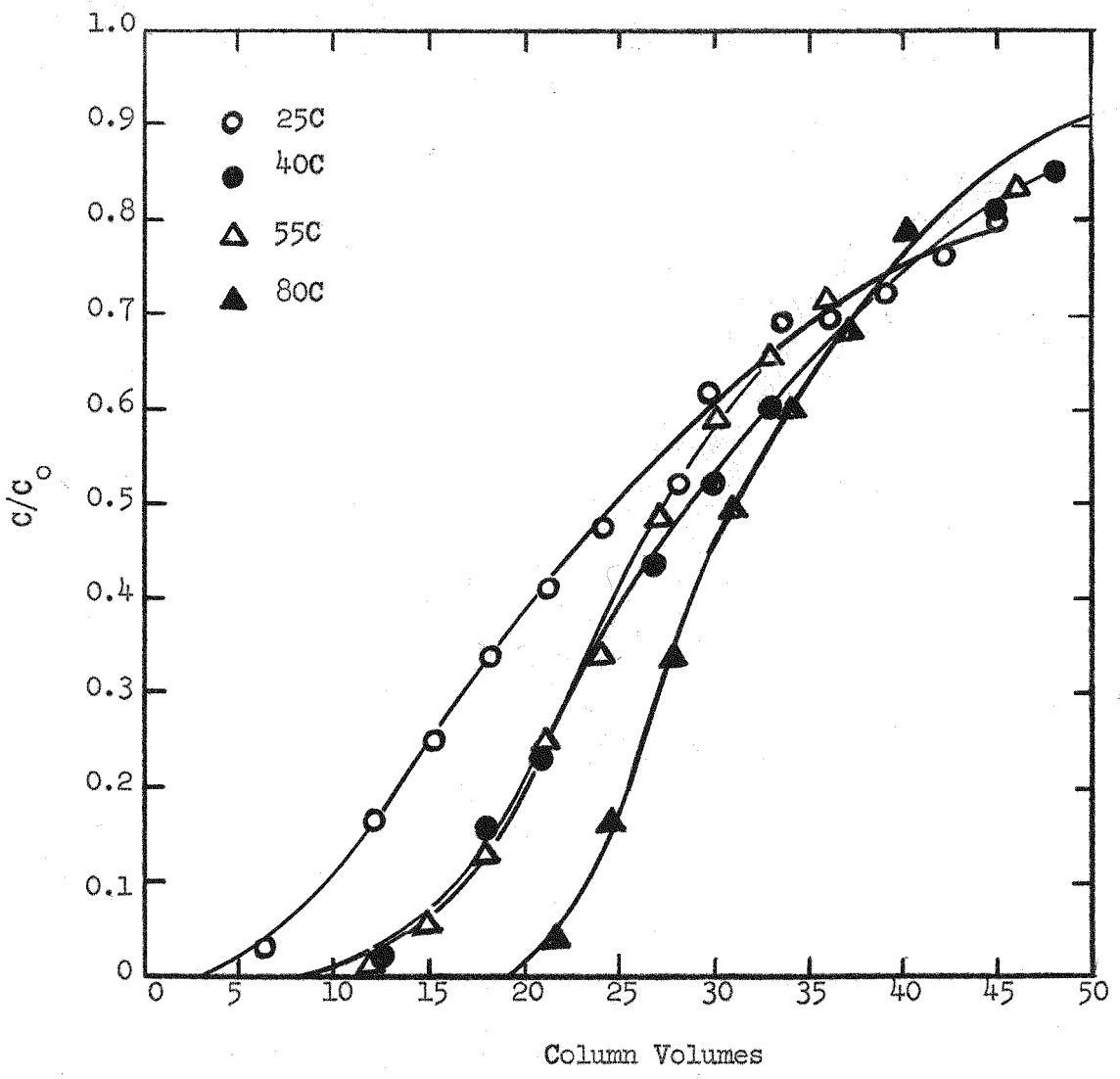

Figure 79. Effect of temperature on strontium breakthrough curves with 4A.

Conditions:

Feed	0.20M $NaNO_3$, 0.035M $Sr(NO_3)_2$, 0.010M $Ca(NO_3)_2$.
Column size	1.9 cm. diameter, 21 cm. height.
Exchanger weight	50 grams
Flow rate	12 c.v./hour
Grain size	20 x 25 mesh

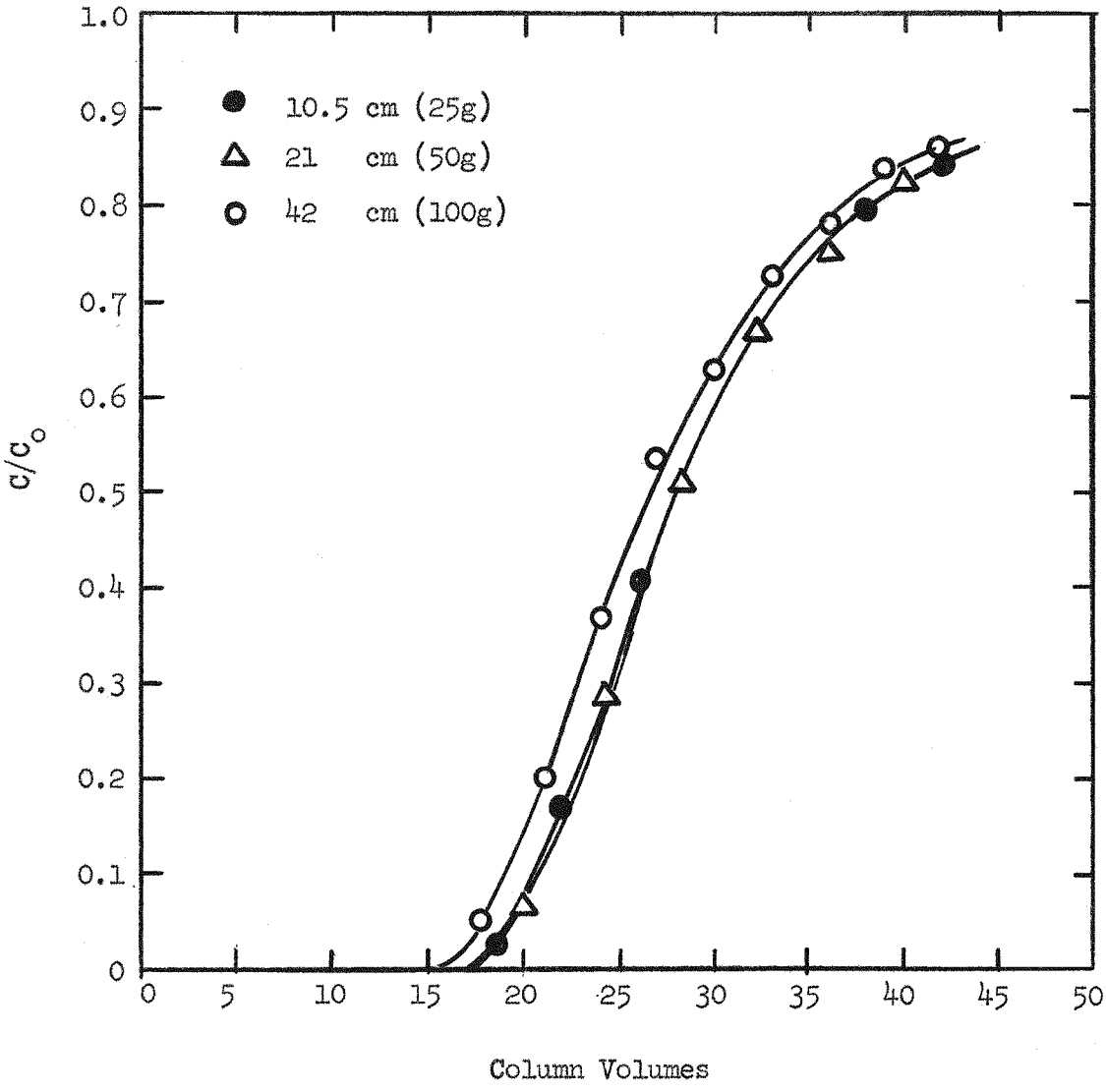

Figure 80. Effect of column height on strontium breakthrough curve with 4A.

Conditions:

Feed	0.20M $NaNO_3$, 0.035M $Sr(NO_3)$, 0.010M $Ca(NO_3)_2$
Column diameter	1.9 cm
Flow rate	6 c.v/hour
Temperature	25C
Particle size	20 x 50 mesh

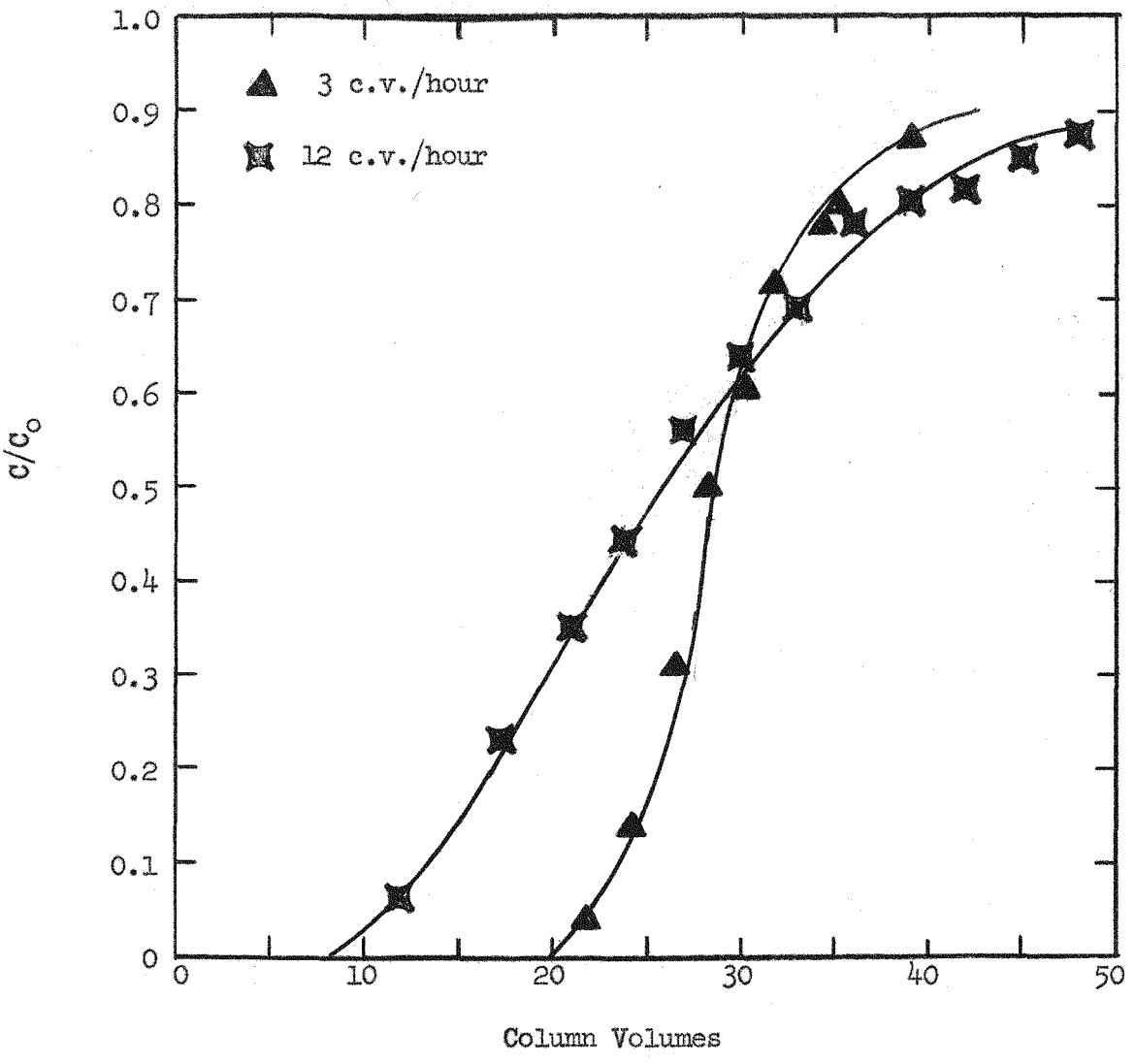

Figure 81. Effect of flow rate on strontium breakthrough curve.

Conditions:

Feed	0.20M $NaNO_3$, 0.035M $Sr(NO_3)_2$, 0.010M $Ca(NO_3)_2$.
Column size	1.9 cm diameter, 21 cm. height.
Exchanger weight	50g.
Temperature	25C
Particle size	30 x 35 mesh.

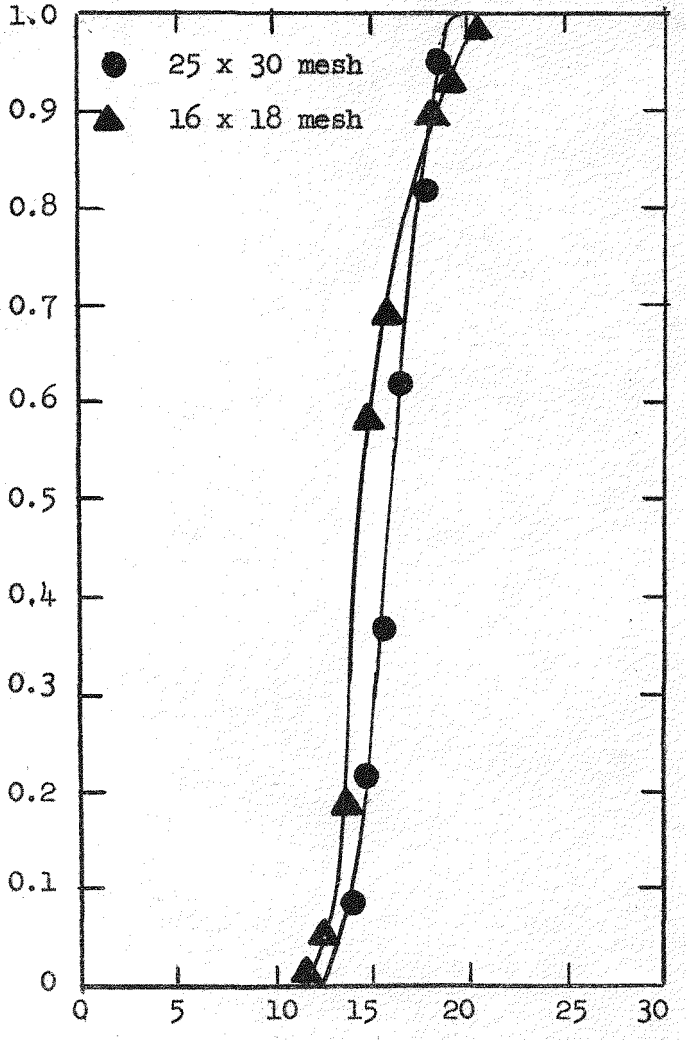

Figure 82 AW-400

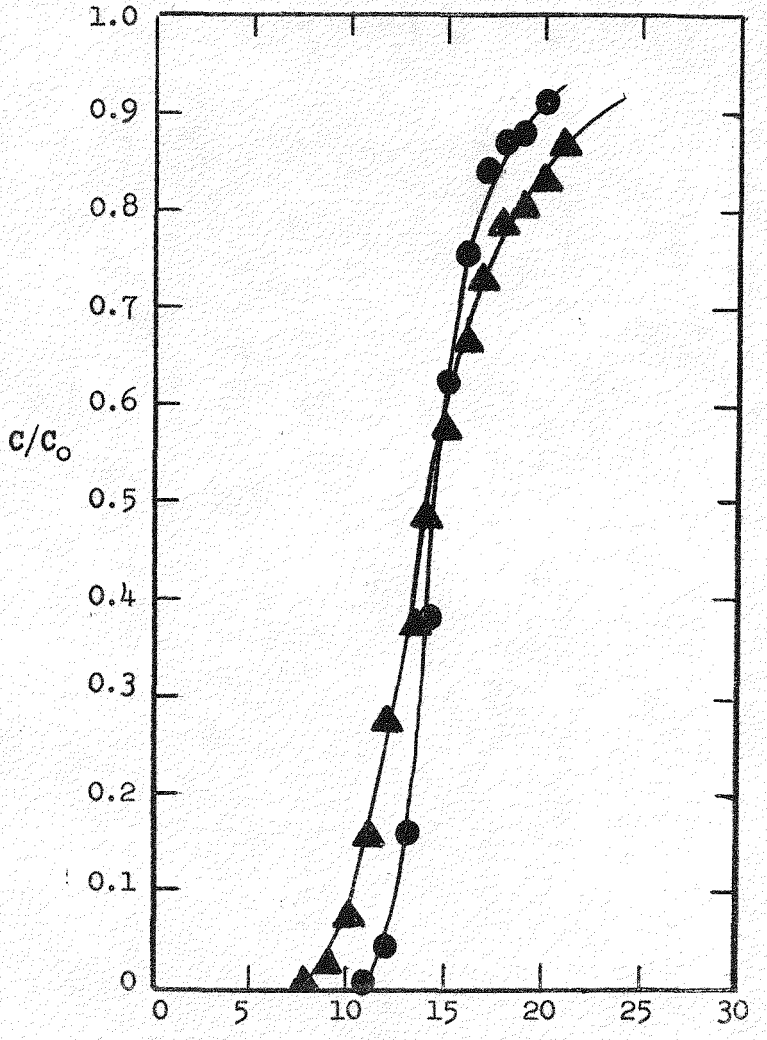

Figure 83 AW-400

Figures 82 and 83. Effect of particle size on cesium breakthrough curve with AW-400 and AW-500.

Conditions

Feed	0.32M Na_2CO_3, 0.04M Cs_2CO_3
Flow rate	4 c.v./hour
Column size	1.9 cm. diameter, 21 cm. height
Exchanger weight	50 grams
Temperature	25C

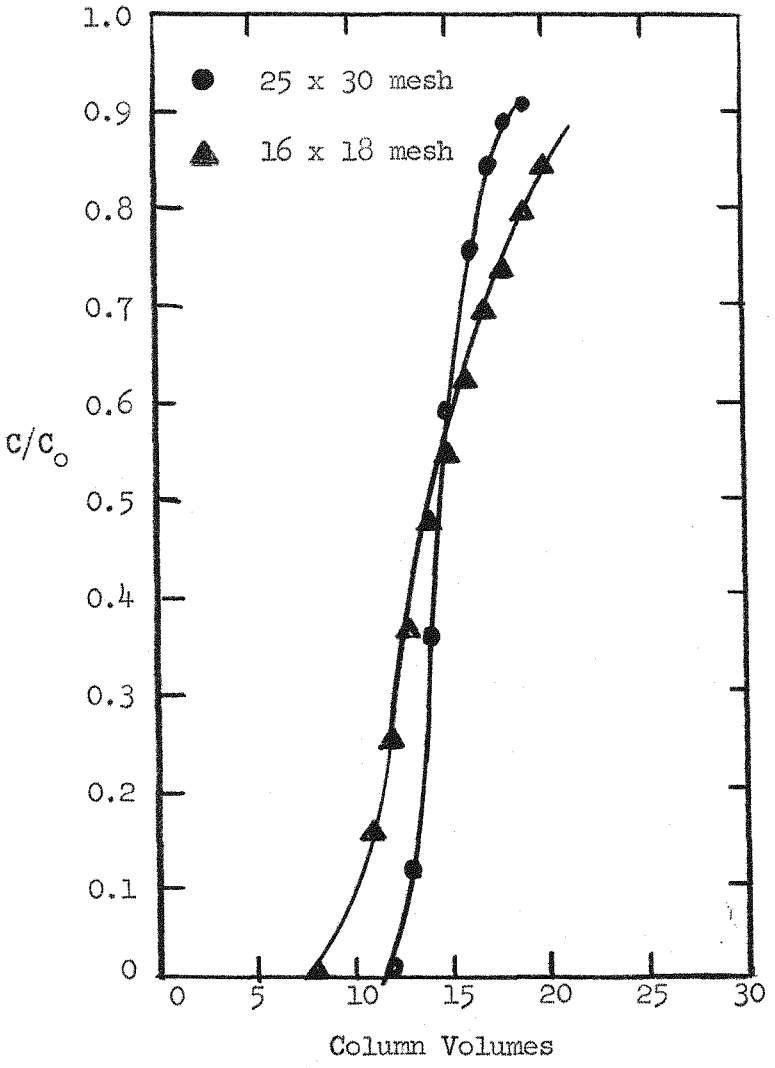

Figure 84 Clinoptilolite

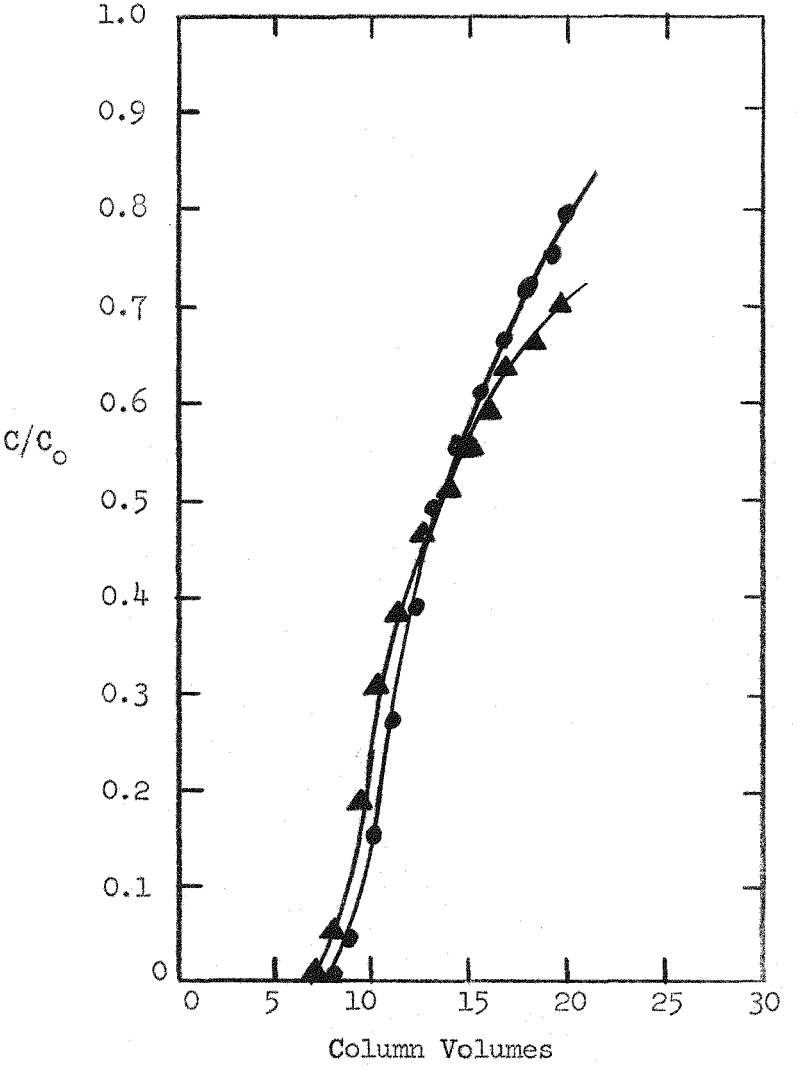

Figure 85 Zeolon

Figures 84 and 85. Effect of particle size on cesium breakthrough curves with clinoptilolite and Zeolon.

Conditions:

Feed	0.32M Na_2CO_3, 0.04M Cs_2CO_3
Flow rate	4 c.v./hour
Column size	1.9 cm. diameter, 21 cm. height
Exchanger weight	50 grams
Temperature	25C

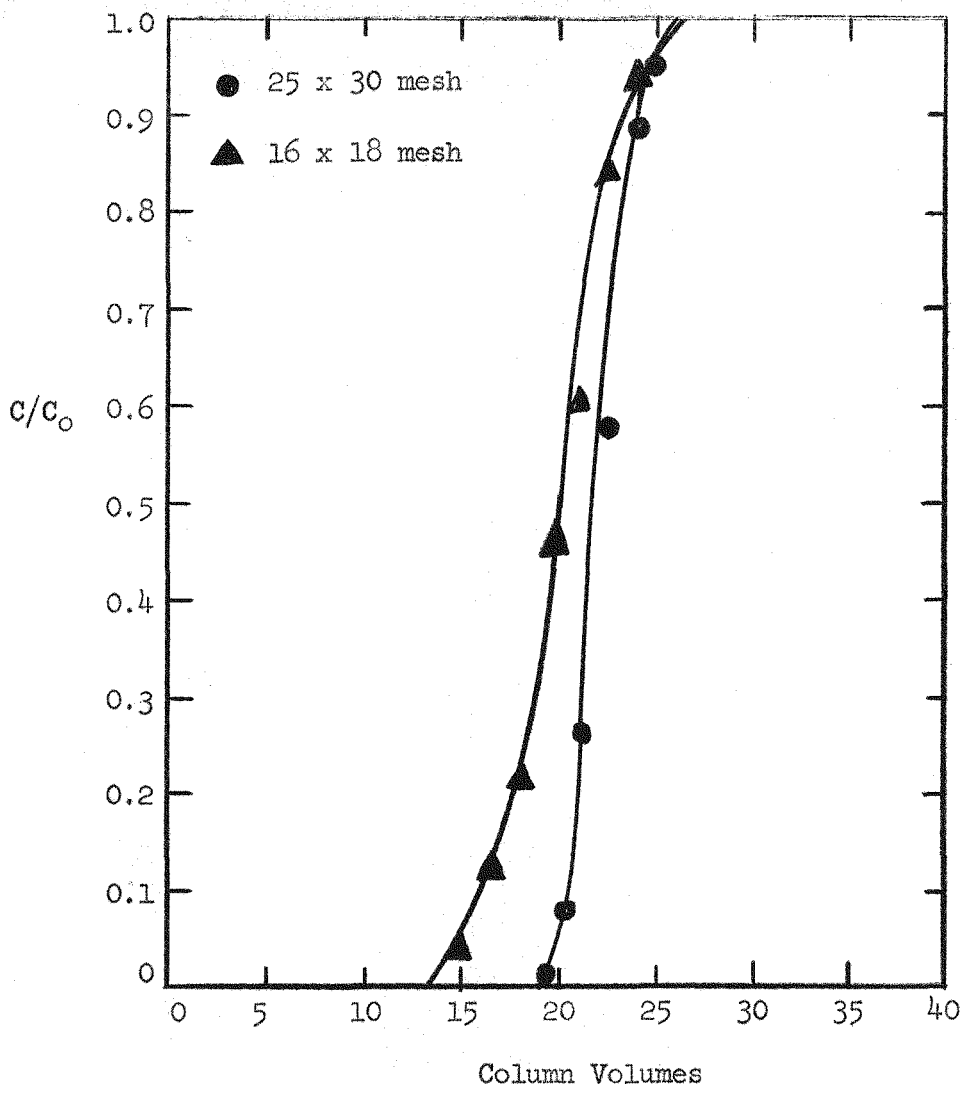

Figure 86. Effect of particle size on cesium breakthrough curve for AW-400 with high Na^+ to Cs^+ ratio in feed.

Conditions:

Feed:	0.50M Na_2CO_3, 0.0248M Cs_2CO_3, 0.005M $(NH_4)_2CO_3$, 0.0125M K_2CO_3.
Flow rate	3 c.v./hour
Column size	1.9 cm. diameter, 21 cm. height
Exchanger weight	50 grams
Temperature	25C

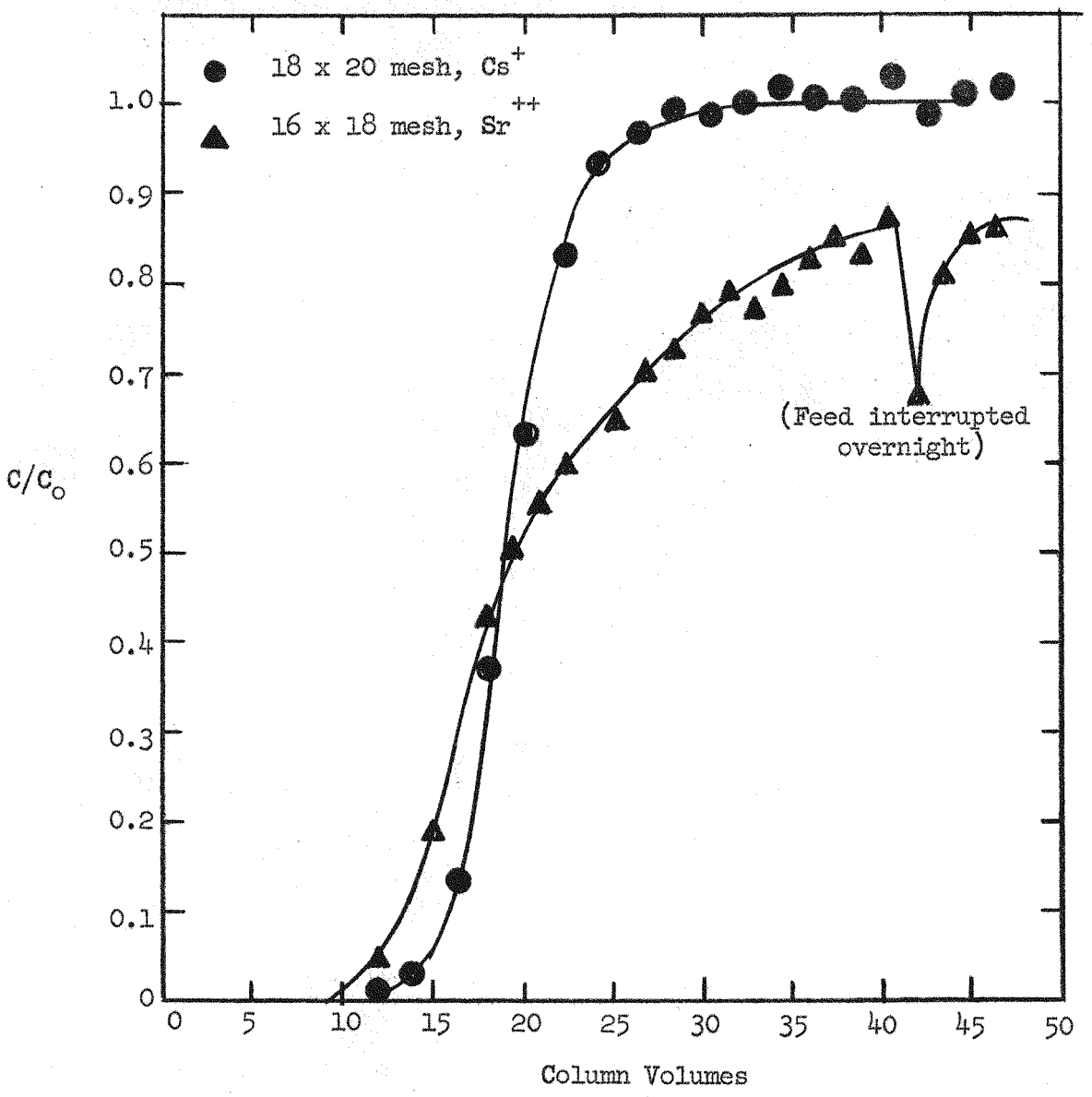

Figure 87. Cesium and strontium breakthrough curves with a simulated CSREX feed and 4A.

Conditions:

Feed	0.20M $NaNO_3$, 0.027M $Sr(NO_3)_2$, 0.027M $Ca(NO_3)_2$, 0.040M $CsNO_3$, 0.001M $Ce(NO_3)_3$, 0.0005M $Nd(NO_3)_2$, 0.005M citrate.
Flow rate	3 c.v./hour
Column size	1.9 cm. diameter, 21 cm. height
Exchanger weight	50 grams
Temperature	25C
pH of feed	5

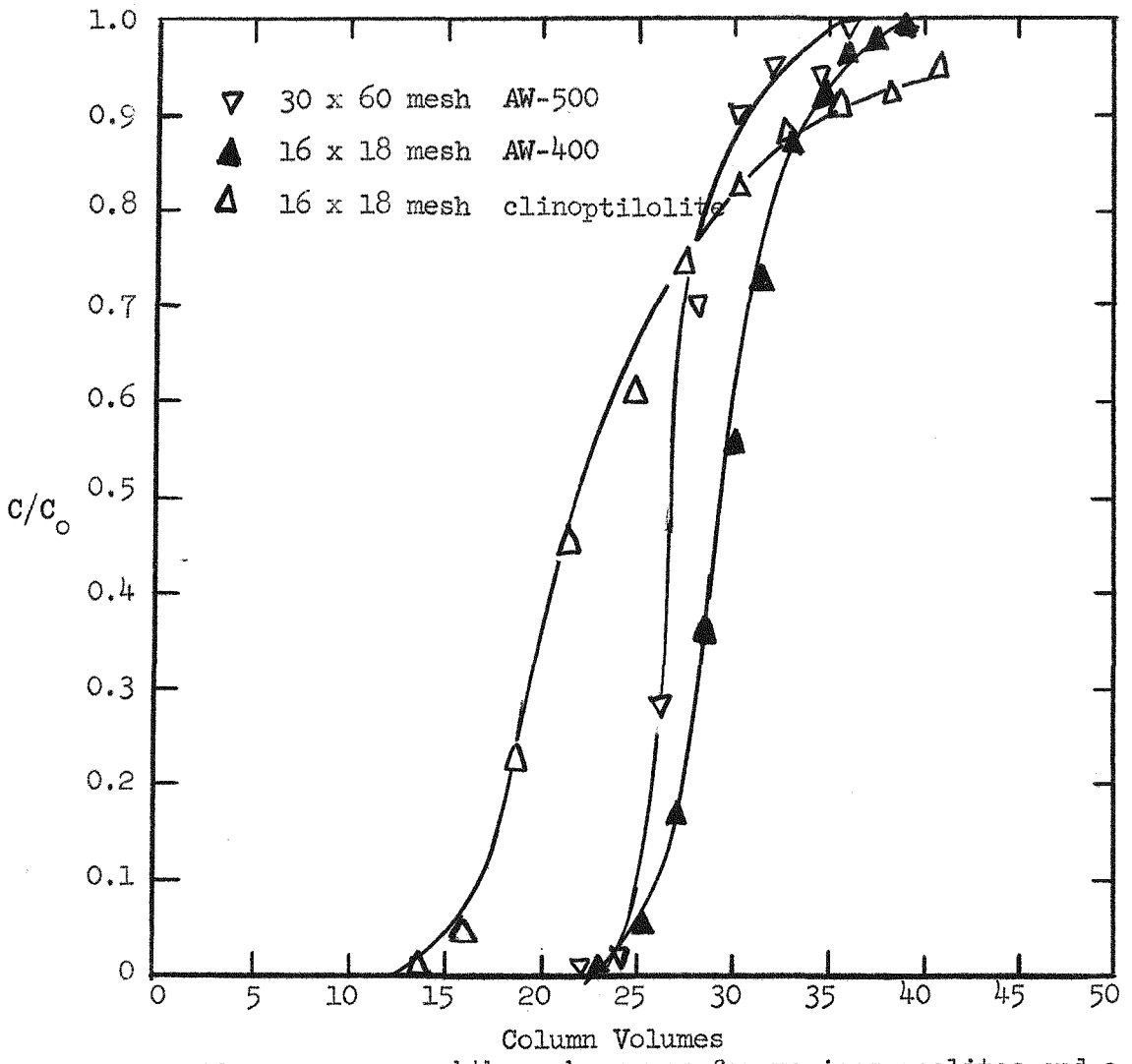

Figure 88. Cesium breakthrough curves for various zeolites and a sumulated CSREX feed.

Conditions:

Feed	0.20M $NaNO_3$, 0.027M $Sr(NO_3)_2$, 0.027M $Ca(NO_3)_2$, 0.040M $CsNO_3$, 0.001M $Ce(NO_3)_3$, 0.0005M $Nd(NO_3)_2$, 0.005M citrate
Flow rate	3 c.v./hour
Column size	1.9 cm. diameter, 21 cm. height
Exchanger weight	50 grams
Temperature	25C
pH of Feed	5

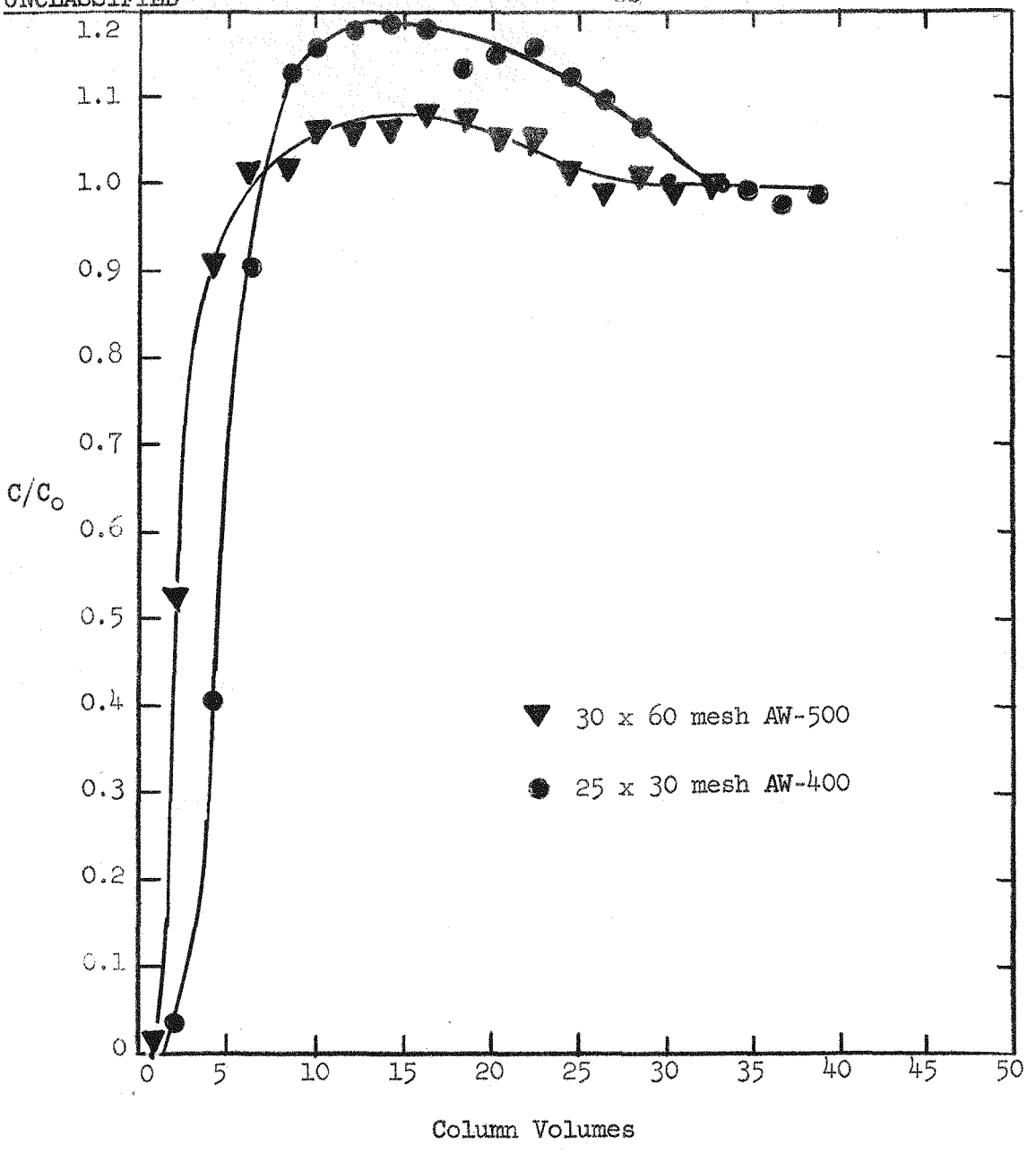

Figure 89. Strontium breakthrough curves for AW-400 and AW-500 with a simulated CSREX feed.

Conditions:

Feed	0.20M $NaNO_3$, 0.027M $Sr(NO_3)_2$, 0.027M $Ca(NO_3)_2$, 0.04M $CsNO_3$, 0.001M $Ce(NO_3)_3$, 0.0005M $Nd(NO_3)_2$, 0.005M citrate.
Flow rate	3 c.v./hour
Column size	1.9 cm. diameter, 21 cm. height
Exchanger weight	50 grams
Temperature	25C
pH of feed	5

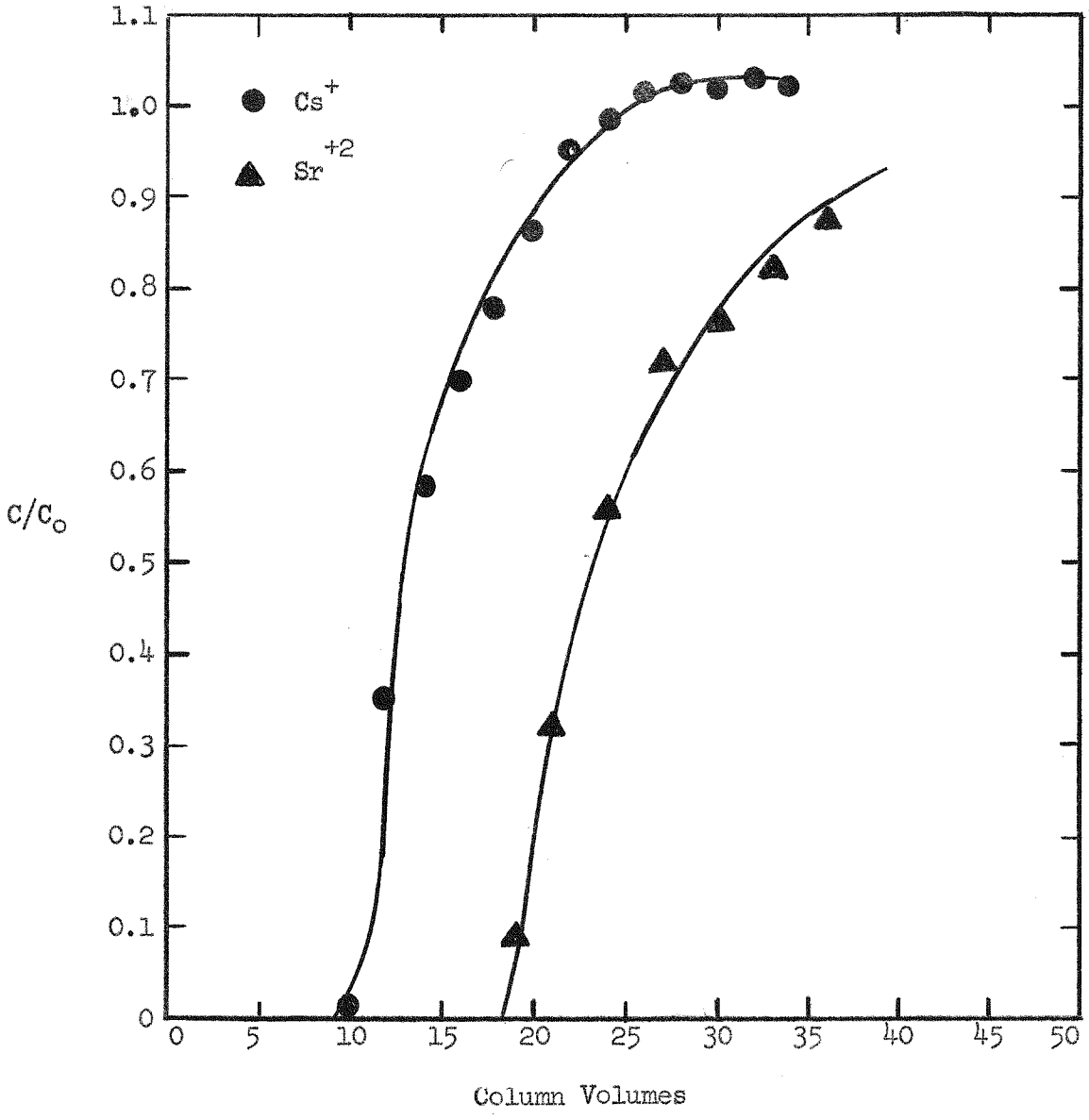

Figure 90. Cesium and strontium breakthrough curves for 4A at 80C with a simulated CSREX feed.

Conditions:

Feed	0.20M, $NaNO_3$, 0.027M $Sr(NO_3)_2$, 0.027M $Ca(NO_3)_2$, 0.040M $CsNO_3$, 0.001M $Ce(NO_3)_3$, 0.0005M $Nd(NO_3)_3$, 0.005M citrate.
Flow rate	12 c.v./hour
Column size	1.9 cm diameter, 21 cm height
Exchanger weight	50g
pH	5
Particle size	30 - 35 mesh

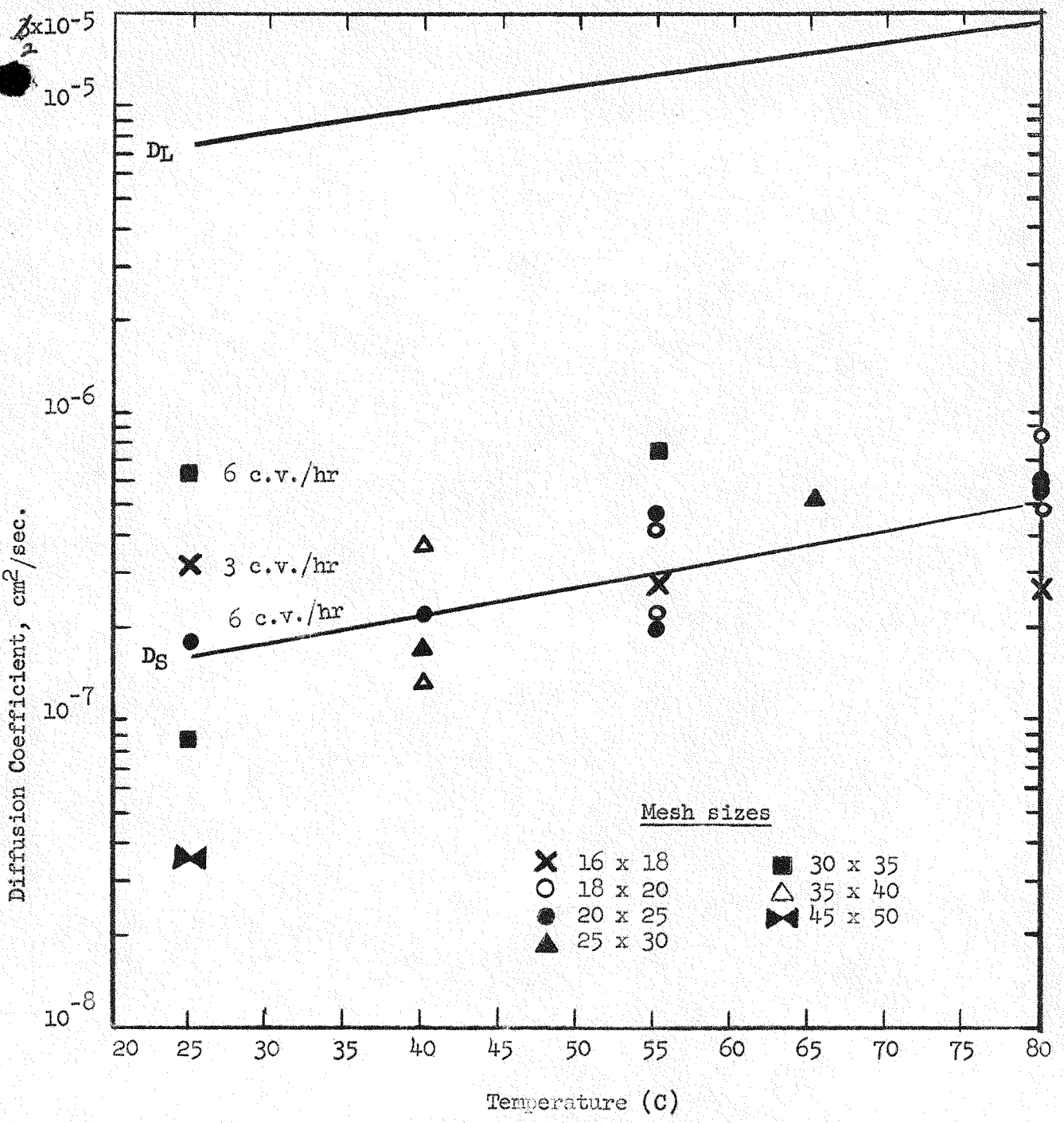

Figure 91. Variation of liquid (D_L) and particle (D_S) strontium diffusion coefficients with temperature for 4A and a simulated D2EHPA 1BP solution.

1BP solution composition: 0.20M $NaNO_3$, 0.035M $Sr(NO_3)_2$, 0.010M $Ca(NO_3)_2$.

Flow rate: 12 c.v./hour unless otherwise indicated.

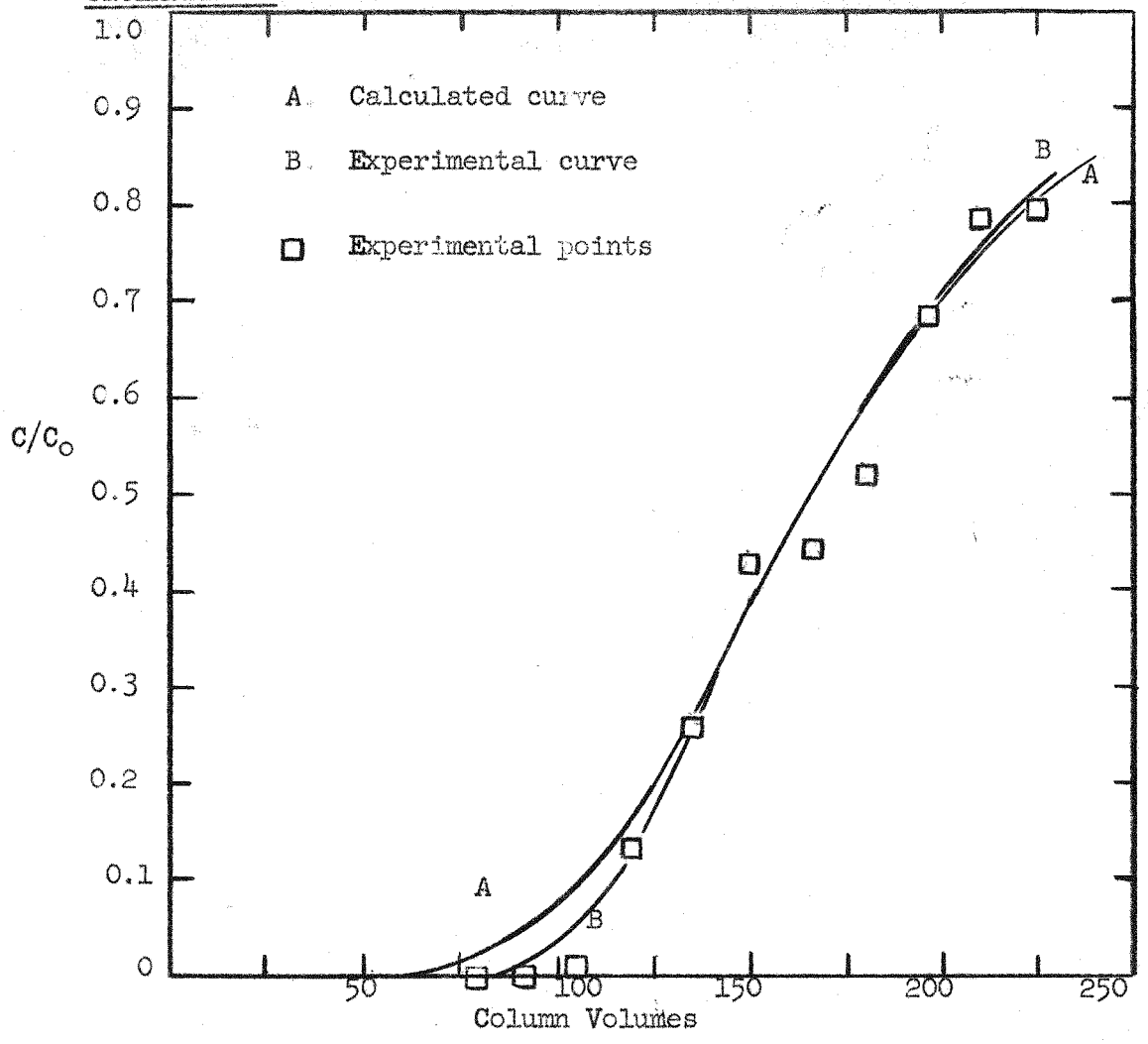

Figure 92. Calculated and experimental strontium breakthrough curves with 4A and dilute feed.

Conditions:

Feed	0.04M $NaNO_3$, 0.007M $Sr(NO_3)_2$, 0.002M $Ca(NO_3)_2$
Flow rate	60 c.v./hour
Column size	1.9 cm. diameter, 21 cm. height
Exchanger weight	50 grams
Temperature	80C
Particle size	20 x 50 mesh

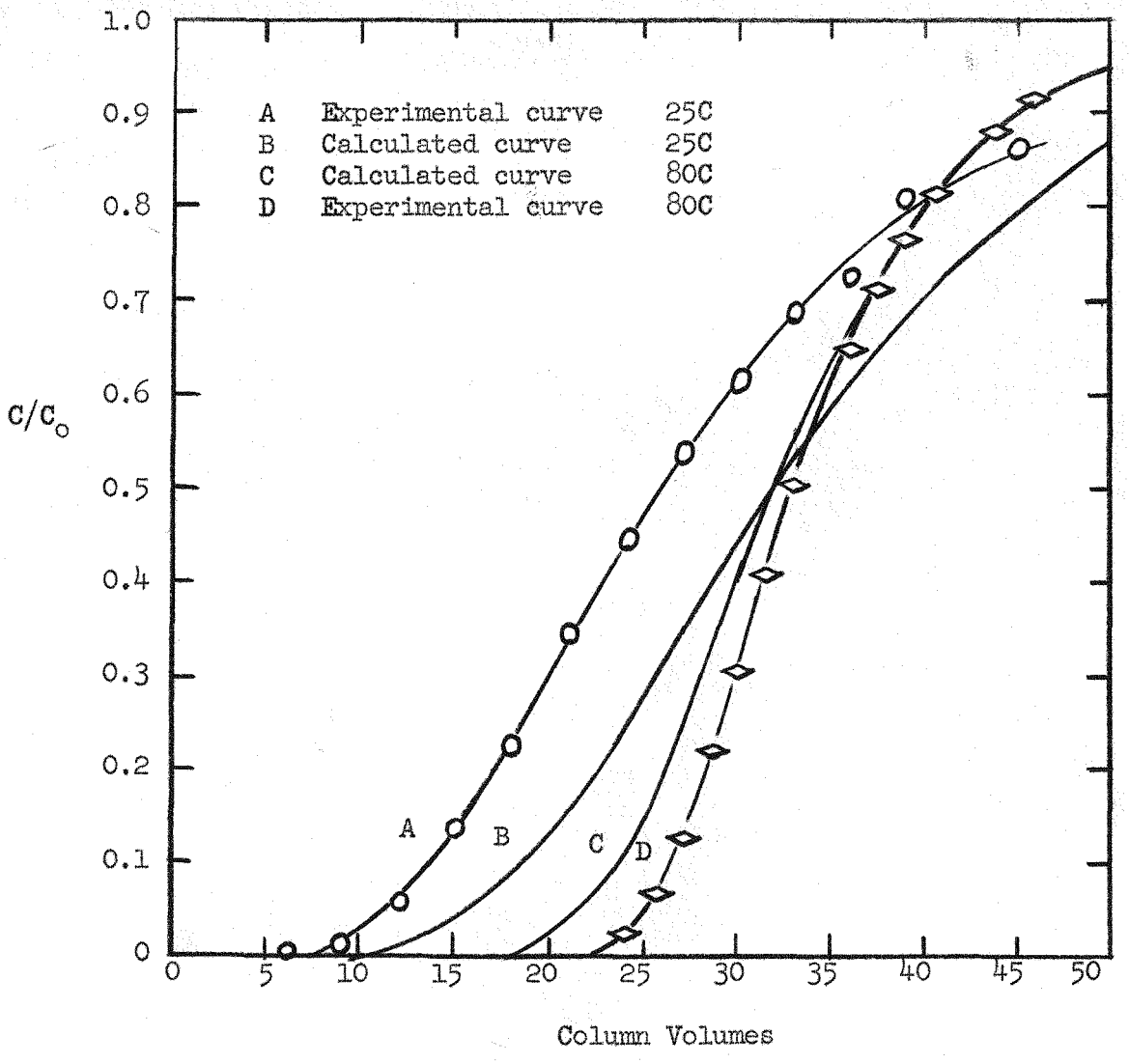

Figure 93. Variations of calculated and experimental strontium breakthrough curves with temperature for 20 x 50 mesh 4A.

Conditions:

Feed	0.20M $NaNO_3$, 0.035M $Sr(NO_3)_2$, 0.010M $Ca(NO_3)_2$
Flow rate	12 c.v./hour
Column size	1.9 cm. diameter, 21 cm. height
Exchanger weight	50g.

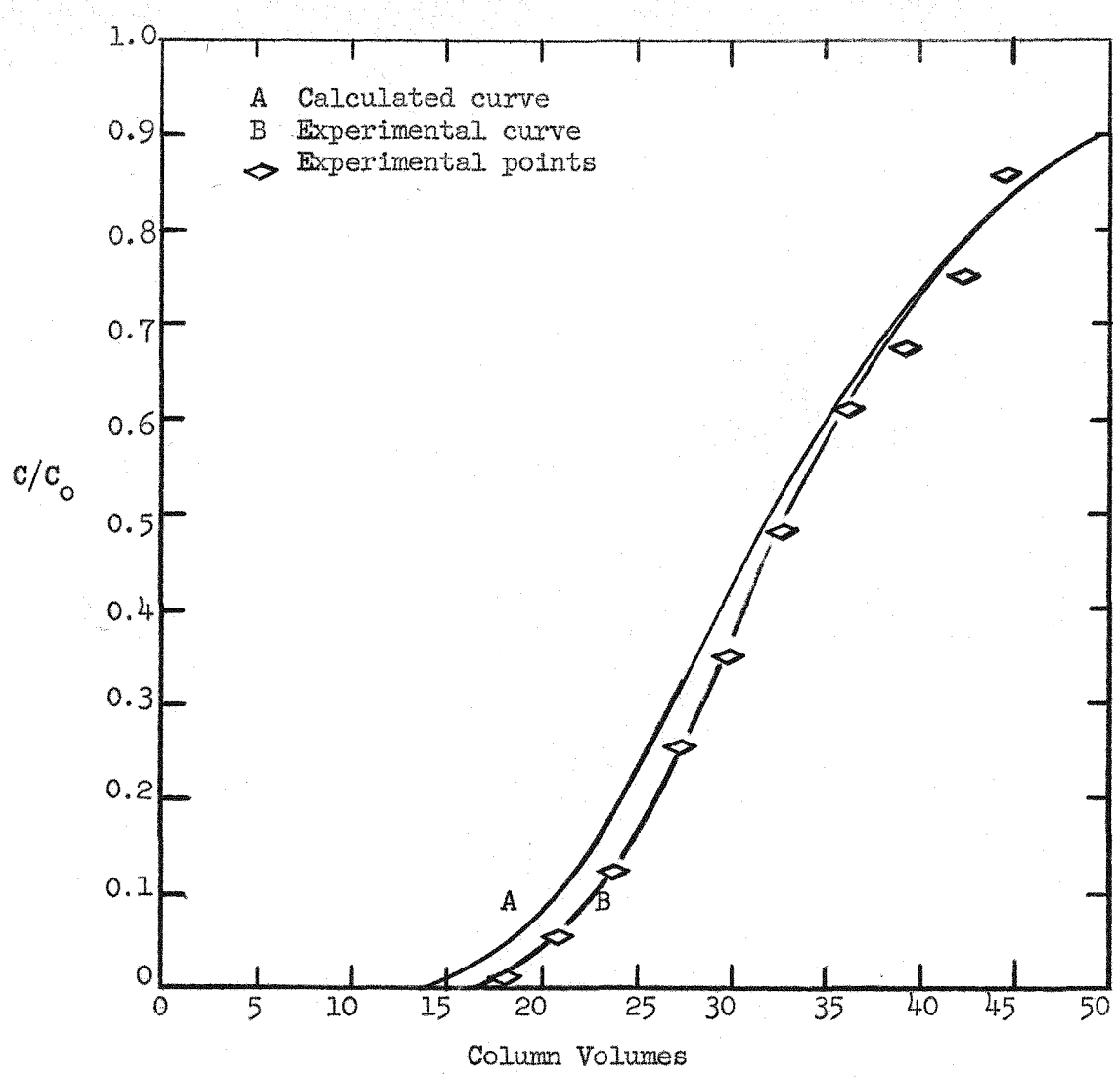

Figure 94. Calculated and experimental strontium breakthrough curves for 14 x 30 mesh 4A.

Conditions:

Feed	0.20M $NaNO_3$, 0.035M $Sr(NO_3)_2$ 0.010M $Ca(NO_3)_2$
Flow rate	12 c.v./hour
Column size	1.9 cm. diameter, 21 cm. height
Exchanger weight	50g.